Title: **Restriction of essential amino acids dictates the systemic response to dietary protein dilution**

Authors: Yann W. Yap[1*], Patricia M. Rusu[1*], Andrea Y. Chan[1], Barbara C. Fam[2], Andreas Jungmann[2,3], Samantha M. Solon-Biet[4], Christopher K. Barlow[5], Darren J. Creek[5,6], Cheng Huang[5], Ralf B. Schittenhelm[5], Bruce Morgan[7], Dieter Schmoll[8], Bente Kiens[9], Matthew D.W. Piper[10], Mathias Heikenwälder[11], Stephen J. Simpson[4], Stefan Bröer[12], Sofianos Andrikopoulos[2], Oliver J. Müller[3, 13], Adam J. Rose[1#]

[1]Department of Biochemistry and Molecular Biology, Metabolism, Diabetes and Obesity Program, Biomedicine Discovery Institute, Monash University, Clayton 3800, Australia.

[2]Department of Internal Medicine III, University Hospital Heidelberg, Heidelberg, Germany.

[3]DZHK (German Centre for Cardiovascular Research), Germany.

[4]Charles Perkins Centre, School of Life and Environmental Sciences, University of Sydney, New South Wales, Australia.

[5]Biomedical Proteomics and Metabolomics Facility and the Department of Biochemistry and Molecular Biology, Biomedicine Discovery Institute, Monash University, Clayton 3800, Australia.

[6]Monash Institute of Pharmaceutical Sciences, Monash University, Melbourne 3052, Australia.

[7]Department of Cellular Biochemistry, University of Kaiserslautern, Kaiserslautern, Germany.

[8]Sanofi-Aventis Deutschland GmbH, Industriepark Hoechst, Frankfurt am Main 65926, Germany.

[9]Section of Molecular Physiology, Department of Nutrition, Exercise and Sports, Faculty of Science, University of Copenhagen, 2100 Copenhagen, Denmark.

[10]School of Biological Sciences, School of Life and Environmental Sciences, Monash University, Clayton, VIC 3800 Australia.

[11]Division Chronic Inflammation and Cancer, German Cancer Research Center, 69120 Heidelberg, Germany.

[12]Research School of Biology, Australian National University, Canberra, 0200, AUS.

[13]Department of Internal Medicine III, University of Kiel, Kiel, Germany.

*equal contribution

#corresponding author

Running title: Requirement of essential amino acid restriction in dietary protein dilution

Abstract (164 words)

Dietary protein dilution (DPD) promotes metabolic remodelling and health but the precise nutritional components driving this response remain elusive. Here we demonstrate that dietary amino acids (AA) are sufficient and necessary to drive the response to DPD. In particular, the restriction of dietary essential AA (EAA) supply, but not non-EAA, drives the systemic metabolic response to total AA deprivation. Furthermore, systemic deprivation of Thr and Trp, independent of total AA supply, are both adequate and necessary to confer the systemic metabolic response to both diet, and genetic AA-transport loss, driven AA restriction. Thr is also potentially limiting in low-protein diet fed humans, and dietary Thr restriction (DTR) retarded the development of obesity-associated metabolic dysfunction in mice. Liver-derived fibroblast growth factor 21 was required for the metabolic remodelling with DTR. Strikingly, hepatocyte-selective establishment of Thr biosynthetic capacity reversed the systemic response to DTR. Taken together, our studies demonstrate that the restriction of EAA are sufficient and necessary to confer the systemic metabolic effects of DPD.

Introduction. (390 words)

The current classification of essential amino acids (EAA) is based on the nutritional requirements for growth and vitality under nil dietary supply of an amino acid (AA) [1]. However, humans rarely face dramatic protein/AA insufficiency, and for the first time in human history, nutritional excesses mean the amount of overweight people outnumber the amount of underweight people on a global scale [2]. This calls for a reconsideration of AA functions in nutrition, now based upon health-related criteria. One approach is dietary protein dilution (DPD), where protein is reduced and replaced by other nutrient sources, and is distinct from caloric restriction [3-6]. Unlike severe protein/AA restriction, which is not compatible with vitality, moderate DPD promotes longevity in multiple species including flies [7-9], rodents [4,10,11] and perhaps humans [12]. Furthermore, DPD also affects health-span and preclinical studies have demonstrated that DPD can retard age-related disease such as cancer [12,13], type 2 diabetes [14,15], and dyslipidemia/fatty liver disease [16,17]. Notably, dietary protein intake rates are positively related to type 2 diabetes risk as well as all-cause mortality in humans [18,19].

While metabolic health and longevity pursuant to DPD is likely to involve numerous mechanisms, it was recently demonstrated that DPD promotes metabolic and physiological adaptations via constituent AA [14,20,21], which is largely mimicked by a genetic deficiency in intestinal and kidney neutral AA transport [22]. In particular, dietary protein or AA restriction promotes such metabolic remodeling and health by the liver-derived hormone fibroblast growth factor 21 (FGF21) [23], largely by increasing energy expenditure relative to food energy intake [14,17,24-32]. Importantly, DPD also increases FGF21 in humans [14,21,24,33], and this increase is associated with heightened energy expenditure [33] and improved indices of metabolic health [14]. However, whether the simultaneous increase in other non-protein/AA nutrients such as certain carbohydrates [34-36] are required for DPD effects, as well as which particular AA drive this process is currently debated [23,37]. On one hand, restriction of EAA such as the branched chain

amino acids [21,38-41] and sulphur-containing AAs [42-45], have been shown to be sufficient in conferring the systemic effects of DPD. On the other hand, others have demonstrated that altered somatic non-EAA metabolism is sufficient and necessary for DPD effects [14,46-49]. Here we attempted to resolve this issue by formally testing which particular amino acids are required to induce the systemic response to DPD.

Results (2422 words)

We previously demonstrated that dietary protein dilution (DPD) improves glucose and lipid homeostasis in obesity and that dilution of amino acids was sufficient to mimic these effects [14,16,49]. However, it remained to be resolved whether the dilution of protein by substituting with other dietary nutrients (i.e. carbohydrate and fat), and/or which particular dietary amino acids, were responsible. To examine this, we fed mice a protein restricted diet (5% energy from casein protein) and compared the effects to a diet where the reduced protein component was replaced with proteinogenic amino acids (AA) at ratios found within casein (see Suppl. Table 1 & 2 for diet compositions). This experiment demonstrated that AA add-back reversed the effects of protein restriction to reduce serum urea (Fig. 1A), a biomarker of general protein/AA supply, establishing that addition of purified amino acids functioned physiologically as protein equivalents. Furthermore, AA-add back to a protein restricted diet reversed the depressed feed efficiency (Figure 1B), as calculated from higher body mass gain despite lower food intake (Suppl. Fig.1B-C). This altered feed efficiency was reflected in an opposite pattern in energy expenditure (EE; Fig. 1C), as gauged from O_2 consumption (Fig. 1D) and CO_2 production (Fig. 1E) rates, with no differences in respiratory exchange ratio (RER; Suppl. Fig. 1D). The increase in EE with DPD occurred independently from differences in body mass during measurement as judged by ANCOVA (Fig. 1F; Adjusted means: NP 0.786±0.005W, LP: 0.955±0.05W, LP+AA: 0.798±0.04W; LP vs NP or LP+AA: $p < 0.001$). The higher EE could not be explained by altered physical activity (Fig. 1G). Consistent with the notion that increased circulating FGF21 is obligatory for the effects of DPD to increase EE [14,16,24,26], we found highly elevated levels of blood plasma FGF21, which were reversed by AA-add back (Fig. 1H). As increased blood FGF21 levels also confer the effects of DPD on improved glucose metabolism [14,49], we also assessed this by measuring an index of fasting insulin sensitivity (ISI(f)) (Fig. 1I) from both fasting glucose (Suppl. Fig. 1E) and insulin (Suppl. Fig. 1F), which correlates well with

improved glucose metabolism with DPD [14]. The increased ISI(f) with DPD was indeed completely reversed with AA-add back (Fig. 1I).

While this experiment demonstrated that AA could be a necessary component of these effects, dietary carbohydrate was concomitantly manipulated, and could potentially explain the responses as FGF21 is affected by certain dietary carbohydrates [31,34-36]. In addition, the specific AA conferring the effects of DPD were not identified. As the liver is an essential organ involved in 'sensing' DPD [14,26], we initially investigated the hepatic portal vein (Fig. 2A; Suppl. File 1) and liver (Fig. 2B; Suppl. File 1) AA levels in response to DPD. While most nutritional [1] essential amino acids (EAA) were lower in the portal vein plasma and liver with DPD, certain non-essential AAs (NEAA) such as Asn, Pro, Glu and Tyr were also affected meaning that we had to take a more broader approach than just focussing on one class of AA. In order to examine this, we conducted a study where we manipulated the EAA and NEAA specifically, on the basis of nutritional definitions [1,50], and in some diets topping up the alternate source of AA to keep the total AA supply constant without altering dietary fat or carbohydrate supply (Fig. 2C). Of note, NEAA supply positively correlated with serum urea more so than EAA supply (Suppl. Fig. 2A), and there were non-binary relationships between EAA/NEAA supply and feed efficiency (Fig. 2D, Suppl. Fig. 2B-C). However, EAA rstriction fully conferred the effects of DPD on EE (Fig. 2E) and serum FGF21 levels (Fig. 2F). In particular, serum FGF21 levels were inversely related to total EAA supply (Fig. 2F).

In this study, we also conducted glucose tolerance tests to further examine diet effects on whole-body metabolism. The blood glucose excursion (Fig. 2G) and related area under the curve (Suppl. Fig. 2D) was directly related to EAA supply, with lower glucose levels found

with EAA restriction. Similar results were seen for that of insulin (Fig 2H & Suppl. Fig. 2E). From fasting glucose (Suppl. Fig. 2F) and insulin (Suppl. Fig. 2G) values, we could calculate various indices of glucose metabolic control such as the ISI(f) (Fig. 2I) and HOMA-IR (Suppl. Fig. 2H). In addition, we calculated the product of the glucose and insulin AUCs (Suppl. Fig. 2I). Importantly, there were very close correlations between the indices determined from fasting glucose and insulin compared with those determined from the glucose tolerance tests (Suppl. Fig. 2J-L). All of these indices highlighted that glucose metabolism/insulin sensitivity is heightened with dietary EAA restriction.

By way of follow-up, we then sought to determine which particular EAA could confer these effects and selected subgroups based upon known biochemical features [50]. In particular, we chose one subgroup based on their classification as ones which cannot be synthesised by any possible precursor within the mammalian metabolic network (i.e. strictly metabolically essential; Lys, Thr, Trp), the branched-chain AA (i.e. Ile, Leu, Val), and the remaining three (i.e. His, Met, Phe). We then conducted studies where we added these EAAs back to the low EAA diet and notably it was only the strictly metabolically essential AA, namely Lys, Thr, and Trp, which were necessary to confer the systemic metabolic effects to total EAA deprivation (Fig. 3A-D & Suppl. Fig. 3A-E).

In an attempt to investigate whether a single one of these EAAs could confer the effects of dietary EAA restriction (DEAR), we then individually added back either Lys, Thr, or Trp to the EAA restricted diet and could demonstrate that no single one of these was necessary for the effects of DEAR (Suppl. Fig. 3F-I). By logical deduction, this meant that restriction of at least two, and perhaps all three, of these EAA were necessary for the full effects of DEAR. To

initially test this, we then conducted a study where we singly restricted Lys, Thr, or Trp, at levels matching those found in the complete AA restriction, and could demonstrate that deprivation of either Thr or Trp, but not Lys, was sufficient to mimic the effects of DEAR (Fig. 3E-H; Suppl. Fig. 3J-N). Importantly, this finding was independently supported in separate experiments whereby a diet low in Met, Thr and Trp induced feed inefficiency and increased serum FGF21 similar to DPD (Suppl. Fig. 3O-R).

To test the necessity of the deprivation of these two EAA for the effects of DEAR, we then conducted studies with selective add-back of these two EAA in the background of a low total AA supply, and could demonstrate that deprivation of both Thr and Trp were required for the systemic metabolic effects of DEAR (Fig 3I-L; Suppl. Fig. 3S-W). In summary, in the background of total dietary protein/AA restriction simultaneously low levels of Thr and Trp are required for the full effects, whereas restriction of either Thr or Trp individually can mimic the majority of effects of DPD.

Our prior studies were done on male mice from 8wks of age, which could potentially limit the applicability of our findings, as female mice are known to respond differently to dietary challenges [51-53], and such young mice are still growing and thus may differ in dietary AA requirements compared with adult mice. Hence, we tested several diets used previously (Fig. 1-3) on 6mo old male and female mice for a longer time frame (i.e. 8wks) to assess potential differences (Fig. 4). Moreover, we tested the effects of total dietary AA restriction (LAA), as well as EAA (LEAA) and threonine (LT) restriction with matched total AA supply, on various parameters such as body composition, metabolic efficiency, and indices of metabolic health. Of note, while LAA and LEAA caused weight loss (LAA) or weight stabilisation (LEAA) (Fig.

4A-B), mostly reflected as lean mass loss, and there was no lean mass loss with LT (Suppl. Fig. 4A-B). This was reflected by end-point tissue weights, with both skeletal muscle and heart weights showing a similar trend to that of lean mass measured by MRI (Fig. 4C-D). Concerning fatness, mice on all diets gained fat mass, but there were no statistically significant differences between diets as assessed by MRI, with the exception of males subjected to LT (Fig. 4A-B). However, when individual adipose tissue depots were assessed, both perigonadal and subcutaneous fat depots were lower in male, but not female, mice subjected to dietary AA/EAA restriction (Fig. 4-C-D). Concerning feed efficiency, the responses were similar to that of the changes in body weight, with dietary AA/EAA restriction promoting consistently reduced feed efficiency regardless of sex (Fig. 4E-F). However, LT feeding produced a consistently higher feed efficiency versus other AA restriction groups (Fig. 4E-F), probably owing to the less pronounced effects on lean mass, as there was an equal increase in EE (Fig. 4G-H) and food E intake (Suppl. Fig. 4C-D) in all groups subjected to AA/EAA restriction regardless of sex.

Similar to the food E intake and EE responses, serum FGF21 levels were equally higher in mice subjected to AA/EAA restriction, again regardless of sex (Fig. 4I-J). Glucose metabolism also showed a similar response, with an equally higher insulin sensitivity index (Fig. 4K-L), as discerned from fasting blood glucose (Suppl. Fig. 4E-F) and plasma insulin (Suppl. Fig. 4G-H), in groups subjected to dietary AA/EAA restriction, again regardless of sex.

As dietary protein dilution also affects lipid metabolism [14,17] and the IGF1 axis [12,14], we also assessed these. Serum triglyceride levels were lower with dietary AA/EAA restriction, and this was more pronounced in male than female mice (Suppl. Fig. 4I-J). Serum IGF1 levels were substantially lower with total AA restriction, but not with dietary Thr restriction, with dietary

EAA restriction producing an intermediary response, particularly in male mice (Suppl. Fig. 4K-L).

To reinforce the findings that only certain EAA such as Thr and Trp are important for the effects of dietary EAA restriction, we then wanted to confirm the importance of these EAA in other situations. We re-examined the serum AA response in humans subjected to a natural low protein diet from freely available foodstuffs [14,49], and could demonstrate that the Thr (Fig 5A), but not Lys or Trp (data not shown), serum excursion was blunted in response to an acute low protein meal following a one week adaptation period. Importantly, of this low protein diet, Thr was identified as the most limiting AA (Fig. 5B) when compared to the AA requirements for the body predicted by an exome matching, genome-based method that can predict the most limiting EAA in any diet [20]. Of note, the basis of this prediction is supported by the evidence that systemic EAA turnover correlates well with EAA exome enrichment [54].

In addition to this, we utilised a mouse model with intestinal and renal neutral amino acid transport deficiency (i.e. B^{0}AT1/Slc6a19 knockout mouse), which exhibits metabolic features akin to dietary protein/AA restriction [22]. Initially, we characterised the hepatic portal vein AA profile, and could demonstrate that while there were higher levels of certain AA such as Arg and Lys, there was substantially lower levels of Thr and Trp (Fig. 5C). In order to test the involvement of these AA in the phenotype of these mice, we conducted an acute AA add-back study, and could demonstrate that systemic add-back (by intraperitoneal administration) of Thr and Trp, but not His and Phe, could reverse the upregulation of blood plasma FGF21 levels in these mice (Fig. 5D), highlighting the importance of these two EAA in the response to dietary AA restriction. Lastly, as we have previously shown that dietary protein or AA dilution can

retard the development of obesity-related metabolic dysfunction, we then tested whether selective Thr restriction (LT), without total AA restriction or altered dietary carbohydrate supply, can mimic these effects in a mouse model of obesity-related metabolic dysfunction, the New Zealand Obese (NZO) mouse. Of note, similar to our prior findings of NZO mice subjected to dietary protein/AA dilution [14,49], there was no effects of LT on body mass development and liver and adipose tissue weights (Suppl. Fig. 5A-B). However, LT completely retarded the development of hyperglycaemia (Fig. 5E), reduced hypertriglyceridemia (Fig. 5F), and increased serum FGF21 levels (Fig. 5G), in this model. Altogether, these results highlight that dietary Thr is a common EAA mediating effects of dietary AA restriction across models and species, and that dietary Thr restriction can affect positive health outcomes in obesity.

As FGF21 was commonly affected by dietary EAA restriction (Fig. 3-5), and liver-derived FGF21 conveys the metabolic remodelling with DPD [14,24,26] and methionine restriction [42], we tested the requirement of liver-derived FGF21 in the systemic metabolic remodelling with LT. As such, we administered adeno-associated viruses to express Cre-recombinase (AAV-CRE) to Fgf21 floxed mice to silence Fgf21 expression/secretion in a liver/hepatocyte specific manner. Indeed, serum levels of FGF21 were absent in groups treated with AAV-CRE (Fig. 6A). Hepatocyte Fgf21 silencing retarded the depressed feed efficiency with LT (Fig. 6B), mostly owing to a complete abrogation of the effects on reduced body mass gain with LT (Suppl. Fig. 6A-B), with blunted effects of LT feeding on fat tissue (Suppl. Fig. 6C). In addition, the effects of LT to increase energy expenditure (Fig 6C; Suppl. Fig. 6D) and food energy intake (Suppl. Fig. 6E) were also abrogated with liver Fgf21 silencing. In congruence, the improved glucose metabolism (Fig. 6D; Suppl. Fig. F-G) and reduced serum triglyceride levels (Suppl. Fig. 6H) with LT were also abrogated with liver/hepatocyte Fgf21 loss. In summary, the systemic metabolic remodelling with LT requires liver-derived FGF21.

Although EAA systemic metabolic turnover is intimately related to genome-wide exome EAA abundance [54], the major metabolic fate of EAA may not be for protein synthesis [50]. Thus, we sought to test whether it is the inability to synthesise the strictly EAA that characterises them as the most limiting and thus required for the effects of DEAR. To this end we produced adeno-associated viruses to express the yeast Thr biosynthetic enzymes (i.e. yTHR1 and yTHR4) in the liver hepatocytes of mice and subjected them to LT. Using high-resolution mass spectrometry, the yeast proteins THR1 and THR4 were confidently identified in mouse liver extracts overexpressing THR1 and THR4, but not of those expressing GFP (Suppl. Fig. 7A; Suppl. File 2). Liver-specific expression was also confirmed by qPCR (data not shown). Importantly, the reduction of liver Thr concentration was reverted with liver-specific enforcement of de novo threonine biosynthesis (Suppl. Fig. 7B; Suppl. Table 3). Strikingly, the effects of dietary Thr restriction on metabolic efficiency, serum FGF21, and glucose metabolism were completely reversed by artificially increasing the liver Thr de novo biosynthesis (Fig. 7; Suppl. Fig. 7).

Discussion (1814 words)

Dietary protein dilution (DPD) promotes metabolic health by inducing the hepatokine fibroblast growth factor 21 (FGF21) [14,16], but the precise nutritional components driving this response are not fully defined. In particular, in order to keep total caloric supply neutral, which is an important consideration in diet-phenotype interactions [3,5], another macronutrient source must be concomitantly increased. In former studies [5,14,24], this was typically achieved by increasing dietary carbohydrates, which may be an independent driver of increased FGF21 [34,35]. DPD can also increase food intake, but particularly on low protein-high-carbohydrate diets, this increased food intake is surpassed by heightened energy expenditure, promoting a situation of systemic metabolic inefficiency [14,24]. However, on a low-protein-high-fat diet, mice gain more body weight [4,14], which may [4] or may not [14,16] promote worsened metabolic health. This weaker response to differing diluting nutrients in DPD is perhaps due to the absence of relatively weaker satiating effects of lipids versus protein or carbohydrate [55,56]. Nevertheless, pair-feeding studies have shown that the DPD-driven heightened energy expenditure and FGF21 can be uncoupled from food intake [32], indicating that the major driver of metabolic inefficiency is not due to food intake.

Importantly, our studies here (Fig. 1-7), as well as previous studies of amino acid (AA) restriction [23,37], have conclusively shown that a restriction of dietary protein/AA *per se* can induce the systemic metabolic response to dietary protein dilution. Even though dietary protein as a nutrient can be digested and absorbed as AA or short peptides, our data reinforce that dietary AA supply is paramount under conditions of dietary protein restriction. Importantly, metabolomic studies of postprandial plasma amino acid levels in Slc6a19 null mice, which mimic the effects of DPD, also revealed a prominent effect on Thr and Trp when fed standard

laboratory chow [57]. By contrast, ablation of intestinal peptide transport does not mimic the effects of DPD [58].

So could restriction of certain AA confer this response? There are several studies showing that dietary essential amino acid (EAA) restriction are sufficient to induce many of the responses to DPD [20,37]. On the other hand, there are several lines of evidence that restriction of systemic non-EAA (NEAA) supply to the liver influences FGF21 and systemic metabolism [14,46-48]. Thus, with the evidence that both EAA and NEAA supply (i.e. hepatic portal vein) and liver AA levels are affected by DPD (Fig 2), we sought to systemically investigate the role of EAA and NEAA restriction. Through a series of studies, we empirically determined that EAA, and in particular the EAA Thr and Trp, are necessary and sufficient to induce the systemic metabolic response to DPD (Fig. 2-7), independent of total dietary AA supply. Importantly, this validates a prior study predicting that Thr is the most limiting AA from AA exome matching under a casein based diet [20] as well as a recent study demonstrating that the hyperphagia due to dietary casein/AA restriction relates to Thr and/or Trp supply [59]. However, here we demonstrate that both Thr and Trp are equally limiting in the casein-based diet through empirical investigation, both by dietary AA restriction and by using a genetic model of AA-transport deficiency (Fig. 5). While this may seem contrary to those studies which have shown that restriction of certain EAA such as the branched chain AA (BCAA) or sulphur-containing AA (SCAA) are sufficient to mimic systemic metabolic response to DPD [37], this may be explained by titration thresholds dictated by ratios of dietary supply and somatic demand. In particular, with regard to titration, basing the deprivation levels on the 5%E casein diet simply identifies those AA most limiting in this natural protein source, and that if we also restricted an AA to a theoretical level below which they would be limiting according to some somatic constraint [20], then this would likely trigger a similar response. Indeed, even though Lys is an abundant AA in the milk protein

casein, it is the most limiting AA in protein derived from maize (i.e. zein) [60], and the dietary supply of many EAAs are reduced in health-promoting vegan diets [61]. Nonetheless, it is known that certain EAA can be synthesised/spared by metabolism of precursors that can be mobilised within the body and/or supplied by diet [50], and thus we propose that it is the strictly metabolically EAA, namely Lys, Thr and Trp, which will most likely be limiting in nearly all foodstuffs. In support of this contention, systemic responses to restriction of the EAA Met can be alleviated by dietary Cys-driven methionine sparing [62-64] and liver refurbishment of *de novo* biosynthesis of Thr abated the effects of dietary Thr restriction (Fig 7). In any case, further studies are required to carefully dissect which EAA drive (mal)-adaptive processes during DPD, and in particular which do so under circumstances of altered somatic AA metabolism such as age-related disease, infection, or pregnancy.

Most of the studies here were conducted using young (i.e. 8wk) male mice fed for a short period of time (i.e. 3 wk). Thus, this may limit the applicability of the findings, especially since female mice can respond differently to dietary challenges [51-53] and AA requirements can be different during growth/maturation versus adulthood [50]. However, the majority of the effects of dietary AA restriction seen in young mice (i.e. feed efficiency, energy expenditure, food intake, glucose metabolism) were also reflected in older male and female mice, albeit with female mice responding to a smaller extent (Fig. 4). Of note however, were the effects of the different AA restriction diets on lean body mass and skeletal/heart muscle mass with total AA or EAA restriction lowering lean tissue mass, whereas the low Thr diet did not. This highlights that a low Thr diet can induce many of the positive effects of dietary AA restriction while avoiding some negative side effects such as lean tissue wasting. On this, similar to that previously shown for dietary protein/AA dilution [14,16,21,49,65], and SCAA or BCAA restriction [21,38,42-44], low Thr feeding also retarded development of obesity-induced metabolic dysfunction in a mouse model

(Fig. 5). Dietary Thr restriction may thus be an attractive strategy to mimic the effects of dietary protein dilution without unwanted caveats, particularly as dietary Thr is largely metabolised by the intestine [66] and thus many potential undesirable systemic side-effects may be avoided.

Several studies have demonstrated that systemic [14,16,24,25,32,40,44,65] or liver-restricted [14,26] Fgf21-loss retards the downstream metabolic effects of dietary protein/AA restriction. In particular, these effects are likely to be mediated by central nervous system FGF21 signalling [65], to stimulate nutrient uptake/oxidation in adipose tissue and heart [14,16]. Here we extend upon these findings and demonstrate that adult, liver-specific FGF21 loss completely abrogates the systemic metabolic remodelling with dietary Thr restriction (Fig. 6). In addition, given that liver/hepatocyte specific restoration of EAA biosynthesis could rescue effects of EAA restriction (Fig. 7), taken together this reinforces the prior evidence [14] that the liver is the chief anatomical site 'sensing' dietary protein/AA restriction which is logical given its proximal anatomical position to nutrient absorption.

In conclusion, the restriction of EAA, particularly Thr and Trp, are sufficient and necessary to confer the systemic metabolic effects of dietary protein dilution.

Methods.

All unique materials are available from commercial vendors or from the authors pending material transfer agreements. The data that support the findings of this study are available from the corresponding author upon reasonable request.

Diets. Diets were purchased either from Specialty Feeds (Perth, AUS; Supplementary Table 1) or Research Diets (New Jersey, USA; Supplementary Table 2). Study A (Fig. 1 and Suppl. Fig. 1) was a comparison of diets SF17-180 (20% E from protein), SF17-175 (5% E from protein) and SF17-176 (5%E from protein and 15%E from amino acids). Study B (Fig. 2C-I and Suppl. Fig. 2) was a comparison of amino acid containing diets A14011601-A14011606). Study C (Fig. 3A-D and Suppl. Fig. 3A-E) was a comparison of diets A14011601, A14011605, and A16120501- A16120503. Study D (Suppl. Fig. 3F-I) was a comparison of diets A14011601, A14011605, and A17020901-A17020903. Study E (Fig 3E-H and Suppl. Fig. 3J-N) was a comparison of diets A14011601, A14011605, and A170401301-A170401303. Study F (Suppl. Fig. 3O-R) was a comparison of diets SF14-162 and SF17-114. Study G (Fig 3I-L and Suppl. Fig. 3S-W) was a comparison of diets SF17-177, SF18-109 and SF17-110. Study H (Fig 4 and Suppl. Fig. 4) was a comparison of diets SF17-177, SF18-109, SF19-086, and SF17-179. Study I (Fig. 5E-G and Suppl. Fig. 5) and study J (Fig. 6 and Suppl. Fig. 6) was a comparison of diets SF17-177 and SF17-179. Study K (Fig. 7 and Suppl. Fig. 7) was a comparison of diets SF17-177 and SF18-066.

Recombinant viruses. A control (green fluorescent protein: GFP), Cre-recombinase, yeast (*Saccharomyces cerevisiae*) Threonine 1 (yTHR1), or Threonine 4 (yTHR4) cDNAs were cloned into AAV genome plasmids for subsequent production of self-complimentary adeno-

associated viruses (AAV) using the three plasmid system. The genome plasmid encoding either hepatocyte specific regulated (via LP1-promoter [67,68]) GFP, yTHR1 or yTHR4 was co-transfected with the adenoviral helper plasmid pDGΔVP and the capsid plasmid p5E18VD2/8-mut6 (aa 589-592: QNTA to GNRQ; AAV8 to AAV2) [69]. Purification and quantification of the final vector stocks was done as described previously [70].

Mouse experiments. Unless stated otherwise, male mice aged 7 weeks upon arrival, were acclimated to the local housing facility (12-12h light-dark cycle, 22-24°C) for one week prior to experimentation and were fed standard rodent chow (3437, Provimi Kliba, DEU or 8720610, Barastoc, AUS) unless otherwise indicated. Mice used for experiments were C57Bl/6NCrl mice (#027, Charles River Laboratories, DEU), C57Bl/6J (Monash University Animal Research Platform, Clayton, AUS or Animal Resource Centre, AUS). Slc6a19-/- and corresponding +/+ littermates [22] as well as Fgf21 fl/fl littermate mice [71] were also used, both on C57Bl/6J background. New Zealand Obese mice [72], a model of obesity-induced type 2 diabetes, were also used.

The dietary intervention was identical for nearly all experiments (Fig. 1, 2, 3, 7) and is outlined in Supplementary Figure 1A. In brief, following acclimation, mice were placed on diets for 3 weeks with body weight recorded each week and metabolic cage housing during week 2 with a 5-h fasting bleed (sometimes with a glucose tolerance test) conducted during week 3 (i.e. day 19-20). Mice were then humanely euthanised for tissue collection.

To examine the chronic effects of dietary AA restriction on fully developed mice, 6mo old male and female C57Bl/6J mice were treated with diets SF17-177 (NAA), SF18-109 (LAA),

SF19-086(LEAA), and SF17-179 (LT) for a period of 8 wks. Body weight and compostion (ECHO-MRI^{TM} 3in1, EchoMRI LLC, USA) was measured before and at the end of the treatment period. Metabolic cage housing was completed for 5d, one-week after diet initiation. A 5h fasting bleed was conducted 7wk after diet initiation. At the end of the 8wk, mice were humanely euthanised for tissue collection.

For studies on New Zealand Obese mice, mice were obtained at 7wk of age and acclimated to the housing facility. At 8wk, they were switched to either diet SF17-177 (NAA) or SF17-179 (LT) and studies for a further 4wk. Mice were weighed and bled for blood glucose measurement in the random fed state before, and each week. At the end of the 8wk, mice were humanely euthanised for tissue collection.

For liver/hepatocyte specific Fgf21 silencing experiments (Fig. 6) we conducted experiments where following acclimation, 7wk old Fgf21fl/fl mice were administered a total of 2.5 x 10^{11} virus particles per mouse via the tail vein. For the negative control (NC): 2.5 x 10^{11} GFP-AAV; and for the Cre-recominase overexpression studies mice were administered 2.5 x 10^{11} virus particles each of CRE-AAV. One week following this time, the dietary intervention was initiated and continued for 8wk with metabolic cage housing during wk 2 and a fasting bleed during wk7. At the end of the 8wk, mice were humanely euthanised for tissue collection.

For liver/hepatocyte specific yTHR1 and yTHR4 expression experiments (Fig. 7), we conducted experiments where following acclimation, mice were administered a total of 5 x 10^{11} virus particles per mouse via the tail vein. For the negative control (NC): 5 x 10^{11} GFP-AAV; and for the THR1/4 overexpression studies mice were administered 2.5 x 10^{11} virus particles

each of yTHR1-AAV and yTHR4-AAV. One week following this time, the dietary intervention was initiated. In these studies, the low threonine diets contained homoserine, the substrate of THR1. Importantly, pilot studies showed no differences in the response to a low threonine diet with or without supplemented homoserine (data not shown).

For the experiment involving selective restriction of Met, Thr and Trp, mice were placed on one of two experimental diets at 12 weeks of age for 6 weeks. Food intake was measured weekly and body weights were measured every 2 weeks. Animals were then humanely euthanised for tissue collection.

Fasting-refeeding experiments were conducted to nutritionally synchronise mice for metabolomics measurement. As such, cohorts of mice was adapted to a control or low protein diet for one week using diets described [14]. After this, they were fasted overnight, and then refed the same diet for 4-5h following which they were anesthetised for hepatic portal vein bleeding (cohort 1) or killed by cervical dislocation for rapid freezing of the liver *in situ* using a freeze clamp precooled in LN_2 (cohort 2).

We conducted hepatic portal vein bleeding from Slc6a19-/- and corresponding +/+ littermate mice with blood serum amino acid profiling as described previously [14]. In order to test for the requirement of systemic Thr and Trp lowering on serum FGF21 in the background of Slc6a19 loss-of-function, we fasted Slc6a19-/- and corresponding +/+ littermates overnight and then refed mice a 20%EP diet for 2h, after which we withdrew the food. Upon food withdrawal, mice were intraperitoneally injected a 0.9% saline solution (Vehicle), or a mixture of L-threonine and L-tryptophan (6 mg each, 12 mg; ~0.5 mg/g body mass), or a mixture of L-

phenylalanine and L-histidine (6 mg each, 12 mg; ~0.5 mg/g body mass) and tail vein blood was then collected 4-5h later.

Animal experiments were conducted according to regional, national, and continental ethical guidelines and approved by local regulatory authorities (Regierungspräsidium Karlsruhe, DEU; Monash University Animal Ethics Committee, AUS; and University of Sydney Animal Ethics Committee, AUS) and conformed to ARRIVE guidelines.

Biometric and metabolic phenotyping. The dietary intervention study is outlined in Supplementary Figure 1A. Mice were housed in groups of 2-3 unless placed within the metabolic cages (see below). Body weight was measured before and after the dietary intervention period and body mass difference was calculated. Indirect calorimetry and food intake was recorded by individual housing in metabolic phenotyping system cages (TSE Phenomaster System (TSE Systems, DEU) or Promethion-M High Definition Multiplexed Respirometry System (Sable Systems International, USA)). Energy expenditure (W) was estimated using the Weir equation [73] from VO_2 and VCO_2 measurements (EE (W or J/s) = ((1.44×(3.94×VO_2 (mL/h) + 1.11×VCO_2 (mL/h))/1000 × 4.196) × 0.28). Feed efficiency was calculated from the quotient of the change in body mass (mg) and food energy intake (kJ) during the metabolic cage housing. To assess whole-body glucose homeostasis, a 5-6h fasting blood sample (fasting initiated at ZT3, sampling at ZT8-9) was collected from the tail vein from which blood glucose (AccuCheck Aviva) and plasma insulin (80-INSMS, Alpco, USA) was measured. In some studies, an intraperitoneal glucose tolerance test was conducted immediately following the fasting blood sample by injection of a fixed dose of 50mg of D-glucose in 0.9% saline [74] with blood samples drawn for glucose and insulin measurement at selected times after. In addition, a fasting insulin sensitivity index (ISIf) was calculated and is

a good surrogate index of whole-body glucose homeostasis [14]. The methods for assessment of glucose homeostasis in mice were conducted in accordance with published guidelines [74,75]. Serum FGF21 (MF2100, R&D Systems, USA), urea (Z5030016, Biochain, USA), and triglycerides (TR0100, Sigma-Aldrich, USA) was also measured from the blood serum samples upon sacrifice by cervical dislocation between ZT3-5.

Metabolomics. Livers were cryogenically pulverized (cryopulverization) using a 12-well biopulverizer (BioSpec Products, OK USA Part number 59012MS) according to the manufacturer's instructions. The frozen tissue powder was then weighed and extracted in 20 µL of extraction solvent (0°C) per mg of tissue. The mixture was then briefly vortexed before sonication in an ice-water bath for 10 minutes followed by centrifugation (20,000 rcf, 4°C, 10 minutes). The supernatant was then transferred to a mass spectrometry vial for LC-MS analysis. The extraction solvent consisted of 2:6:1 $CHCl_3$:MeOH:H_2O v/v/v with 2 µM CHAPS, CAPS, PIPES and TRIS as internal standards. Additionally where quantitative amino acid analysis was performed, a mixture of stable isotope labelled amino acids were added at a concentration of 500 pmol of each amino acid per mg liver (Cambridge Isotope Laboratories PN MSK-A2-1.2).

Plasma (25 µL) was extracted by addition of 200 µL of 1:1 acetonitrile:MeOH v/v with 1 µM CHAPS, CAPS, PIPES and TRIS as internal standards at 0°C. Samples were then mixed on a vortex mixer for 30 minutes at 4°C after which they were centrifuged (20,000 rcf, 4°C, 15 min) and the supernatant then transferred to a mass spectrometry vial for LC-MS analysis.

For LC−MS analysis, samples were analyzed by hydrophilic interaction liquid chromatography coupled to high-resolution mass spectrometry (LC−MS) according to a previously published method [76]. In brief, the chromatography utilized a ZIC-pHILIC column (column temperature

25 °C) with a gradient elution of 20 mM ammonium carbonate (A) and acetonitrile (B) (linear gradient time-%B as follows: 0 min-80%, 15 min-50%, 18 min-5%, 21 min-5%, 24 min-80%, 32 min-80%) on a Dionex RSLC3000 UHPLC (Thermo). The flow rate was maintained at 300 µL/min. Samples were kept at 4 °C in the autosampler and 10 µL injected for analysis. The mass spectrometry was performed at 35 000 resolution (accuracy calibrated to <1 ppm) on a Q-Exactive Orbitrap MS (Thermo) operating in rapid switching positive (4 kV) and negative (−3.5 kV) mode electrospray ionization (capillary temperature 300 °C; sheath gas 50; Aux gas 20; sweep gas 2; probe temp 120 °C). All samples were analyzed in randomized order and with pooled quality control samples analyzed regularly throughout the batch to confirm reproducibility. ~300 metabolite standards, including all reported amino acids, were analyzed immediately preceding the batch to determine accurate retention times to confirm metabolite identification.

For data analysis, untargeted metabolomics data were analyzed using the IDEOM (version 20) workflow with default parameters [77]. In brief, this involved peak picking with XCMS [78], peak alignment and filtering with mzMatch [79] and further filtering, metabolite identification, and comparative analysis with IDEOM. Amino acid concentration was determined by integration of the extracted ion chromatograms of the amino acids and their corresponding stable isotope labelled isotopologues in MZmine 2.32 [80,81]. All peaks were inspected and where necessary the integration parameters altered to insure accurate integrations. Nearly all the amino acids were detected in both polarities, however we elected to use the negative mode data for all amino acids except Ala, Arg, Gly and His where we used positive mode data. The amino acid concentration was then calculated by comparison of the peak areas of each amino acid against its corresponding heavy labelled isotopologue.

Proteomics. The mouse liver tissue was homogenized in liquid nitrogen using a BioPulverizer and directly solubilized in SDS (sodium dodecyl sulfate) lysis buffer. The protein concentration was determined using a BCA kit (Thermo Scientific) and equal amounts of protein were processed for both pooled control (GFP) and THR1/4-overexpressed mouse liver sample. SDS was removed by chloroform/methanol precipitation and the proteins were proteolytically digested with trypsin (Promega) and purified using OMIX C18 Mini-Bed tips (Agilent Technologies) prior to LC-MS/MS analysis. Using a Dionex UltiMate 3000 RSLCnano system equipped with a Dionex UltiMate 3000 RS autosampler, an Acclaim PepMap RSLC analytical column (75 µm x 50 cm, nanoViper, C18, 2 µm, 100Å; Thermo Scientific) and an Acclaim PepMap 100 trap column (100 µm x 2 cm, nanoViper, C18, 5 µm, 100Å; Thermo Scientific), the tryptic peptides were separated by increasing concentrations of 80% ACN / 0.1% formic acid at a flow of 250 nl/min for 158 min and analyzed with a QExactive Plus mass spectrometer (Thermo Scientific) using in-house optimized parameters to maximize the number of peptide identifications. To obtain peptide sequence information, the raw files were searched with Byonic v3.0.0 (ProteinMetrics) against a mouse UniProt/SwissProt database that was appended with the yeast THR1/THR4 protein sequences. Only proteins falling within a false discovery rate (FDR) of 1% based on a decoy database were considered for further analysis.

RNA extraction and analysis. RNA was extracted from tissues using QIAzol and cDNA was synthesized using the Quantitect Reverse Transcription Kit (Qiagen). qPCR was conducted using Quantitect Sybr Green qPCR (Qiagen) with the following primers: PrimePCR™ SYBR® Green Assays to yeast Thr1 and Thr4 (Biorad) as well as mouse Tbp (Quantitect, Qiagen) as a housekeeping gene.

Human studies. Details of the study in humans have been published previously [14]. Dietary amino acid content of the of the low protein diet was calculated according to Dankost 3000 (Dankost ApS, Copenhagen, Denmark) and compared against the amino acid distribution in the human exome as previously described [20].

Statistical analyses. Mice were assigned to groups based upon initial body mass for counterbalancing. Pre-established criteria for exclusion of mice from study groups were obvious infections/wounds which would impact on feeding behaviour as well as metabolic profile. Where possible, analysis of data collection was blinded.

Statistical analyses were performed using t-tests (two-sided), or 2-way analysis of variance (ANOVA) with or without repeated measures, where appropriate, with Holm-Sidak-adjusted post-tests. All analyses were carried out with GraphPad Prism v.7.01 software (GraphPad Software, Inc.) or SigmaPlot 14 (Systat Software, Inc.). Statistical details can be found within the Figure legends. Differences between groups were considered significant when $P < 0.05$.

References

1. Rose, W.C. II. The sequence of events leading to the establishment of the amino acid needs of man. *American journal of public health and the nation's health* **58**, 2020-2027 (1968).
2. Popkin, B.M., Adair, L.S. & Ng, S.W. Global nutrition transition and the pandemic of obesity in developing countries. *Nutr Rev* **70**, 3-21 (2012).
3. Mitchell, S.E., *et al.* The effects of graded levels of calorie restriction: I. impact of short term calorie and protein restriction on body composition in the C57BL/6 mouse. *Oncotarget* **6**, 15902-15930 (2015).
4. Solon-Biet, S.M., *et al.* The ratio of macronutrients, not caloric intake, dictates cardiometabolic health, aging, and longevity in ad libitum-fed mice. *Cell Metab* **19**, 418-430 (2014).
5. Solon-Biet, S.M., *et al.* Dietary Protein to Carbohydrate Ratio and Caloric Restriction: Comparing Metabolic Outcomes in Mice. *Cell reports* **11**, 1529-1534 (2015).
6. Raubenheimer, D. & Simpson, S.J. Protein Leverage: Theoretical Foundations and Ten Points of Clarification. *Obesity (Silver Spring)* **27**, 1225-1238 (2019).
7. Lee, K.P., *et al.* Lifespan and reproduction in Drosophila: New insights from nutritional geometry. *Proc Natl Acad Sci U S A* **105**, 2498-2503 (2008).
8. Piper, M.D., *et al.* A holidic medium for Drosophila melanogaster. *Nat Methods* **11**, 100-105 (2014).
9. Mair, W., Piper, M.D. & Partridge, L. Calories do not explain extension of life span by dietary restriction in Drosophila. *PLoS Biol* **3**, e223 (2005).
10. Ross, M.H. Length of life and nutrition in the rat. *J Nutr* **75**, 197-210 (1961).
11. Miller, D.S. & Payne, P.R. Longevity and protein intake. *Exp Gerontol* **3**, 231-234 (1968).
12. Levine, M.E., *et al.* Low protein intake is associated with a major reduction in IGF-1, cancer, and overall mortality in the 65 and younger but not older population. *Cell Metab* **19**, 407-417 (2014).
13. Fontana, L., *et al.* Dietary protein restriction inhibits tumor growth in human xenograft models. *Oncotarget* **4**, 2451-2461 (2013).
14. Maida, A., *et al.* A liver stress-endocrine nexus promotes metabolic integrity during dietary protein dilution. *J Clin Invest* **126**, 3263-3278 (2016).
15. Kitada, M., *et al.* A low-protein diet exerts a beneficial effect on diabetic status and prevents diabetic nephropathy in Wistar fatty rats, an animal model of type 2 diabetes and obesity. *Nutr Metab (Lond)* **15**, 20 (2018).
16. Maida, A., *et al.* Dietary protein dilution limits dyslipidemia in obesity through FGF21-driven fatty acid clearance. *J Nutr Biochem* **57**, 189-196 (2018).
17. Trevino-Villarreal, J.H., *et al.* Dietary protein restriction reduces circulating VLDL triglyceride levels via CREBH-APOA5-dependent and -independent mechanisms. *JCI insight* **3**(2018).
18. van Nielen, M., *et al.* Dietary protein intake and incidence of type 2 diabetes in Europe: the EPIC-InterAct Case-Cohort Study. *Diabetes Care* **37**, 1854-1862 (2014).
19. Song, M., *et al.* Association of Animal and Plant Protein Intake With All-Cause and Cause-Specific Mortality. *JAMA internal medicine* **176**, 1453-1463 (2016).
20. Piper, M.D.W., *et al.* Matching Dietary Amino Acid Balance to the In Silico-Translated Exome Optimizes Growth and Reproduction without Cost to Lifespan. *Cell Metab* **25**, 1206 (2017).
21. Fontana, L., *et al.* Decreased Consumption of Branched-Chain Amino Acids Improves Metabolic Health. *Cell reports* **16**, 520-530 (2016).
22. Jiang, Y., *et al.* Mice lacking neutral amino acid transporter B(0)AT1 (Slc6a19) have elevated levels of FGF21 and GLP-1 and improved glycaemic control. *Molecular metabolism* **4**, 406-417 (2015).
23. Hill, C.M., Berthoud, H.R., Munzberg, H. & Morrison, C.D. Homeostatic sensing of dietary protein restriction: A case for FGF21. *Front Neuroendocrinol* (2018).

24. Laeger, T., *et al.* FGF21 is an endocrine signal of protein restriction. *J Clin Invest* **124**, 3913-3922 (2014).
25. Laeger, T., *et al.* Metabolic Responses to Dietary Protein Restriction Require an Increase in FGF21 that Is Delayed by the Absence of GCN2. *Cell reports* **16**, 707-716 (2016).
26. Perez-Marti, A., *et al.* A low-protein diet induces body weight loss and browning of subcutaneous white adipose tissue through enhanced expression of hepatic fibroblast growth factor 21 (FGF21). *Mol Nutr Food Res* (2017).
27. Ozaki, Y., *et al.* Rapid increase in fibroblast growth factor 21 in protein malnutrition and its impact on growth and lipid metabolism. *Br J Nutr* **114**, 1410-1418 (2015).
28. Chalvon-Demersay, T., *et al.* Low-protein diet induces, whereas high-protein diet reduces hepatic FGF21 production in mice, but glucose and not amino acids up-regulate FGF21 in cultured hepatocytes. *J Nutr Biochem* **36**, 60-67 (2016).
29. Hu, S., *et al.* Dietary Fat, but Not Protein or Carbohydrate, Regulates Energy Intake and Causes Adiposity in Mice. *Cell Metab* **28**, 415-431 e414 (2018).
30. Bielohuby, M., *et al.* Impaired glucose tolerance in rats fed low-carbohydrate, high-fat diets. *Am J Physiol Endocrinol Metab* **305**, E1059-1070 (2013).
31. Solon-Biet, S.M., *et al.* Defining the Nutritional and Metabolic Context of FGF21 Using the Geometric Framework. *Cell Metab* **24**, 555-565 (2016).
32. Hill, C.M., *et al.* Low protein-induced increases in FGF21 drive UCP1-dependent metabolic but not thermoregulatory endpoints. *Scientific reports* **7**, 8209 (2017).
33. Vinales, K.L., *et al.* FGF21 is a Hormonal Mediator of the Human "Thrifty" Metabolic Phenotype. *Diabetes* (2018).
34. von Holstein-Rathlou, S., *et al.* FGF21 Mediates Endocrine Control of Simple Sugar Intake and Sweet Taste Preference by the Liver. *Cell Metab* **23**, 335-343 (2016).
35. Talukdar, S., *et al.* FGF21 Regulates Sweet and Alcohol Preference. *Cell Metab* **23**, 344-349 (2016).
36. Fisher, F.M., *et al.* A critical role for ChREBP-mediated FGF21 secretion in hepatic fructose metabolism. *Molecular metabolism* **6**, 14-21 (2017).
37. Green, C.L. & Lamming, D.W. Regulation of metabolic health by essential dietary amino acids. *Mechanisms of ageing and development* (2018).
38. Wanders, D., *et al.* Metabolic responses to dietary leucine restriction involve remodeling of adipose tissue and enhanced hepatic insulin signaling. *BioFactors* **41**, 391-402 (2015).
39. Guo, F. & Cavener, D.R. The GCN2 eIF2alpha kinase regulates fatty-acid homeostasis in the liver during deprivation of an essential amino acid. *Cell Metab* **5**, 103-114 (2007).
40. De Sousa-Coelho, A.L., *et al.* FGF21 mediates the lipid metabolism response to amino acid starvation. *J Lipid Res* **54**, 1786-1797 (2013).
41. Du, Y., Meng, Q., Zhang, Q. & Guo, F. Isoleucine or valine deprivation stimulates fat loss via increasing energy expenditure and regulating lipid metabolism in WAT. *Amino Acids* **43**, 725-734 (2012).
42. Wanders, D., *et al.* FGF21 Mediates the Thermogenic and Insulin-Sensitizing Effects of Dietary Methionine Restriction but Not Its Effects on Hepatic Lipid Metabolism. *Diabetes* **66**, 858-867 (2017).
43. Hasek, B.E., *et al.* Dietary methionine restriction enhances metabolic flexibility and increases uncoupled respiration in both fed and fasted states. *Am J Physiol Regul Integr Comp Physiol* **299**, R728-739 (2010).
44. Fisher, F.M., *et al.* Fibroblast growth factor 21 limits lipotoxicity by promoting hepatic fatty acid activation in mice on methionine and choline-deficient diets. *Gastroenterology* **147**, 1073-1083 e1076 (2014).
45. Pissios, P., *et al.* Methionine and choline regulate the metabolic phenotype of a ketogenic diet. *Molecular metabolism* **2**, 306-313 (2013).
46. Cornu, M., *et al.* Hepatic mTORC1 controls locomotor activity, body temperature, and lipid metabolism through FGF21. *Proc Natl Acad Sci U S A* **111**, 11592-11599 (2014).
47. Wilson, G.J., *et al.* GCN2 is required to increase fibroblast growth factor 21 and maintain hepatic triglyceride homeostasis during asparaginase treatment. *Am J Physiol Endocrinol Metab* **308**, E283-293 (2015).

48. Shimizu, N., *et al.* A muscle-liver-fat signalling axis is essential for central control of adaptive adipose remodelling. *Nature communications* **6**, 6693 (2015).
49. Maida, A., *et al.* Repletion of branched chain amino acids reverses mTORC1 signaling but not improved metabolism during dietary protein dilution. *Molecular metabolism* **6**, 873-881 (2017).
50. Reeds, P.J. Dispensable and indispensable amino acids for humans. *J Nutr* **130**, 1835S-1840S (2000).
51. Yu, D., *et al.* Short-term methionine deprivation improves metabolic health via sexually dimorphic, mTORC1-independent mechanisms. *FASEB J* **32**, 3471-3482 (2018).
52. Larson, K.R., *et al.* Sex Differences in the Hormonal and Metabolic Response to Dietary Protein Dilution. *Endocrinology* **158**, 3477-3487 (2017).
53. Medrikova, D., *et al.* Sex differences during the course of diet-induced obesity in mice: adipose tissue expandability and glycemic control. *Int J Obes (Lond)* **36**, 262-272 (2012).
54. Hui, S., *et al.* Glucose feeds the TCA cycle via circulating lactate. *Nature* **551**, 115-118 (2017).
55. Speakman, J.R. Why lipostatic set point systems are unlikely to evolve. *Molecular metabolism* **7**, 147-154 (2018).
56. Simpson, S.J., Le Couteur, D.G. & Raubenheimer, D. Putting the balance back in diet. *Cell* **161**, 18-23 (2015).
57. Javed, K., Cheng, Q., Carroll, A.J., Truong, T.T. & Broer, S. Development of Biomarkers for Inhibition of SLC6A19 (B(0)AT1)-A Potential Target to Treat Metabolic Disorders. *International journal of molecular sciences* **19**(2018).
58. Nassl, A.M., *et al.* Amino acid absorption and homeostasis in mice lacking the intestinal peptide transporter PEPT1. *Am J Physiol Gastrointest Liver Physiol* **301**, G128-137 (2011).
59. Solon-Biet, S.M., *et al.* Branched-chain amino acids impact health and lifespan indirectly via amino acid balance and appetite control. *Nature Metabolism* **1**, 532-545 (2019).
60. Kligler, D. & Krehl, W.A. Lysine deficiency in rats. I. Studies with zein diets. *J Nutr* **41**, 215-229 (1950).
61. Kahleova, H., Fleeman, R., Hlozkova, A., Holubkov, R. & Barnard, N.D. A plant-based diet in overweight individuals in a 16-week randomized clinical trial: metabolic benefits of plant protein. *Nutrition & diabetes* **8**, 58 (2018).
62. Jonsson, W.O., Margolies, N.S. & Anthony, T.G. Dietary Sulfur Amino Acid Restriction and the Integrated Stress Response: Mechanistic Insights. *Nutrients* **11**(2019).
63. Wanders, D., *et al.* Role of GCN2-Independent Signaling Through a Noncanonical PERK/NRF2 Pathway in the Physiological Responses to Dietary Methionine Restriction. *Diabetes* **65**, 1499-1510 (2016).
64. Ball, R.O., Courtney-Martin, G. & Pencharz, P.B. The in vivo sparing of methionine by cysteine in sulfur amino acid requirements in animal models and adult humans. *J Nutr* **136**, 1682S-1693S (2006).
65. Hill, C.M., *et al.* FGF21 Signals Protein Status to the Brain and Adaptively Regulates Food Choice and Metabolism. *Cell reports* **27**, 2934-2947 e2933 (2019).
66. Schaart, M.W., *et al.* Threonine utilization is high in the intestine of piglets. *J Nutr* **135**, 765-770 (2005).
67. Graham, T., McIntosh, J., Work, L.M., Nathwani, A. & Baker, A.H. Performance of AAV8 vectors expressing human factor IX from a hepatic-selective promoter following intravenous injection into rats. *Genetic vaccines and therapy* **6**, 9 (2008).
68. Rose, A.J., *et al.* Molecular control of systemic bile acid homeostasis by the liver glucocorticoid receptor. *Cell Metab* **14**, 123-130 (2011).
69. Raupp, C., *et al.* The threefold protrusions of adeno-associated virus type 8 are involved in cell surface targeting as well as postattachment processing. *J Virol* **86**, 9396-9408 (2012).
70. Jungmann, A., Leuchs, B., Katus, H.A., Rommelaere, J. & Muller, O.J. Protocol for efficient generation and characterization of adeno-associated viral (AAV) vectors. *Hum Gene Ther Methods* (2017).

71. Potthoff, M.J., *et al.* FGF21 induces PGC-1alpha and regulates carbohydrate and fatty acid metabolism during the adaptive starvation response. *Proc Natl Acad Sci U S A* **106**, 10853-10858 (2009).
72. Veroni, M.C., Proietto, J. & Larkins, R.G. Evolution of insulin resistance in New Zealand obese mice. *Diabetes* **40**, 1480-1487 (1991).
73. Weir, J.B. New methods for calculating metabolic rate with special reference to protein metabolism. 1949. *Nutrition* **6**, 213-221 (1990).
74. Andrikopoulos, S., Blair, A.R., Deluca, N., Fam, B.C. & Proietto, J. Evaluating the glucose tolerance test in mice. *Am J Physiol Endocrinol Metab* **295**, E1323-1332 (2008).
75. Ayala, J.E., *et al.* Standard operating procedures for describing and performing metabolic tests of glucose homeostasis in mice. *Dis Model Mech* **3**, 525-534 (2010).
76. Srivastava, A., Evans, K.J., Sexton, A.E., Schofield, L. & Creek, D.J. Metabolomics-Based Elucidation of Active Metabolic Pathways in Erythrocytes and HSC-Derived Reticulocytes. *Journal of proteome research* **16**, 1492-1505 (2017).
77. Creek, D.J., Jankevics, A., Burgess, K.E., Breitling, R. & Barrett, M.P. IDEOM: an Excel interface for analysis of LC-MS-based metabolomics data. *Bioinformatics* **28**, 1048-1049 (2012).
78. Tautenhahn, R., Bottcher, C. & Neumann, S. Highly sensitive feature detection for high resolution LC/MS. *BMC Bioinformatics* **9**, 504 (2008).
79. Scheltema, R.A., Jankevics, A., Jansen, R.C., Swertz, M.A. & Breitling, R. PeakML/mzMatch: a file format, Java library, R library, and tool-chain for mass spectrometry data analysis. *Anal Chem* **83**, 2786-2793 (2011).
80. Pluskal, T., Castillo, S., Villar-Briones, A. & Oresic, M. MZmine 2: modular framework for processing, visualizing, and analyzing mass spectrometry-based molecular profile data. *BMC Bioinformatics* **11**, 395 (2010).
81. Katajamaa, M., Miettinen, J. & Oresic, M. MZmine: toolbox for processing and visualization of mass spectrometry based molecular profile data. *Bioinformatics* **22**, 634-636 (2006).

Author contributions: Study conception: AJR. Study design: AJR & SJS. Reagent design, construction and provision: BCF, AJ, BM, SB, SO, OJM, AJR. Performed experiments: YWY, PMR, AYLC, SMS-B, TPS, BK, MH, AJR. Analysed samples and data: YWY, SMS-B, CKB, DJC, CH, RBS, DS, BK, MWDP, MH, SJS, AJR. Wrote manuscript: AJR. Drafted manuscript: YWY, PMR, SMS-B, CCK, CH, SJS, SB, OJM, AJR.

Acknowledgements: The authors wish to thank former lab members Thomas Gantert and Adriano Maida (German Cancer Research Center, Heidelberg, Germany) who conducted the pilot studies for this study series. The experimental and technical assistance of Robert Lee (Monash Metabolic Phenotyping Facility, Australia), Anja Pfenninger (Sanofi-Aventis, Germany), Annika Zota, Max Schuster, and Sarah Lerch (German Cancer Research Center, Germany) is gratefully acknowledged. These studies were supported by Monash Biomedicine Discovery Institute laboratory start-up funds to AJR as well as a Monash Joint Science-Medicine Interdisciplinary Research Seed Funding to AJR and MDWP.

Figure legends

Figure 1. Dietary amino acids are required for the systemic metabolic effects of dietary protein dilution.

A: Serum urea levels of mice in response to a 3wk treatment with diets containing 20% energy from protein (20P), 5% energy from protein (5P), and 5% energy from protein and 15% energy from amino acids to match that of 20P. n=5 per group.

B: Feed efficiency of mice as in A.

C: Energy expenditure over the different day phases of mice as in A.

D: The rate of O_2 consumption (VO_2) over the different day phases of mice as in A.

E: The rate of CO_2 production (VCO_2) over the different day phases of mice as in A.

F: Scatter plot of energy expenditure (EE) versus body weight of mice as in A.

G: Physical activity as assessed by laser beam breaks across 3 physical dimensions (sumXYZ) over the different day phases of mice as in A.

H: Serum fibroblast growth factor 21 (FGF21) levels of mice as in A.

I: Insulin sensitivity index during fasting (ISI(f)) of mice as in A.

Data are mean and SEM. Different than 20P: * P <0.05, **P<0.01, ***P<0.001. Different than 5P: $^{\#}$P<0.05, $^{\#\#}$P<0.01, $^{\#\#\#}$P<0.001.

Supplementary Figure 1. Dietary amino acids are required for the systemic metabolic effects of dietary protein dilution. Related to Figure 1.

A: Protocol for the diet intervention studies.

B: C: The change (Δ) in body mass of mice in response to a 3wk treatment with diets containing 20% energy from protein (20P), 5% energy from protein (5P), and 5% energy from protein and 15% energy from amino acids to match that of 20P. n=5 per group.

C: The rate of food energy (E) intake during the metabolic cage housing of mice as in B.

D: The respiratory exchange ratio (VCO_2:VO_2) of mice as in B.

E: Fasting blood glucose of mice as in B.

F: Fasting serum insulin of mice as in B.

Data are mean and SEM. Different than 20P: * P <0.05, **P<0.01, ***P<0.001. Different than 5P: $^{\#}$P<0.05, $^{\#\#}$P<0.01, $^{\#\#\#}$P<0.001.

Figure 2. Dietary essential amino acid restriction, independent from non-essential amino acid or carbohydrate supply, dictates the systemic metabolic response to dietary protein dilution.

A: Hepatic portal vein amino acid levels in response to refeeding a low-protein diet following a week of diet adaptation. Data (mean and SEM) are represented at % of the control group fed a normal protein diet (20%P). n=4/group. Different than 20%P, *p<0.05.

B: Liver tissue amino acid levels in response to refeeding a low-protein diet following a week of diet adaptation. Data are represented at % of the control group fed a normal protein diet (20%P). n=4/group. Different than 20%P, *p<0.05.

C: Nutrient source breakdown as % contribution to total energy for the experimental groups. EAA: essential amino acids. NEAA: non-essential amino acids.

D: Feed efficiency of mice in response to a 3wk treatment with diets as per protocol of SF1A containing nutrient energy sources as in C. Data are mean and SEM. Different than diet A: * P <0.05, **P<0.01, ***P<0.001. Different than diet B: $^{\#}$P<0.05, $^{\#\#}$P<0.01, $^{\#\#\#}$P<0.001.

E: Energy expenditure of mice as in D.

F: Serum fibroblast growth factor 21 (FGF21) levels of mice as in D.

G: Blood glucose levels during an intraperitoneal glucose tolerance test (ipGTT) of mice as in D.

H: Plasma insulin levels during an intraperitoneal glucose tolerance test (ipGTT) of mice as in D.

I: Insulin sensitivity index during fasting (ISI(f)) of mice as in D

Supplementary Figure 2. Dietary essential amino acids, independent from non-essential amino acid or carbohydrate supply, dictate the systemic metabolic response to dietary protein dilution. Related to Figure 2.

A: Serum urea of mice in response to a 3wk treatment with diets as per protocol of SF1A containing nutrient energy sources as in Figure 2C. Data (N=5 per group) are mean and SEM. Different than diet A: * P <0.05, **P<0.01, ***P<0.001. Different than diet B: $^{\#}$P<0.05, $^{\#\#}$P<0.01, $^{\#\#\#}$P<0.001.

B: The change (Δ) in body mass of mice over the 3wk intervention as in A.

C: The rate of food energy (E) intake per day during the metabolic cage housing of mice as in A.

D: The glucose area under the curve (AUCg) during an intraperitoneal glucose tolerance test glucose tolerance test of mice as in A.

E: The insulin area under the curve (AUCi) during an intraperitoneal glucose tolerance test glucose tolerance test of mice as in A.

F: Fasting blood glucose of mice as in A.

G: Fasting serum insulin of mice as in A.

H: Homeostatic model assessment of insulin resistance (HOMA-IR) of mice as in A.

I: The product of the glucose and insulin areas under the curve (AUCg*AUCi) an intraperitoneal glucose tolerance test glucose tolerance test of mice as in A.

J: A scatter plot of the fasting insulin sensitivity index (ISI(f))and inverse of the AUCg*AUCi during the intraperitoneal glucose tolerance test glucose tolerance test of mice as in A.

K: A scatter plot of the HOMA-IR and AUCg*AUCi during the intraperitoneal glucose tolerance test glucose tolerance test of mice as in A.

L: A scatter plot of the ISI(f) and during the intraperitoneal glucose tolerance test glucose tolerance test of mice as in A.

Figure 3. Certain essential amino acids including Threonine and Tryptophan are sufficient and necessary for the systemic metabolic effects of dietary protein dilution.

A: Feed efficiency of mice in response to a 3wk treatment with diets containing 18% from amino acids (normal amino acid; NAA), 4.5% essential AA (LEAA; as of diet E in Figure 2C), and LEAA supplemented with either lysine, threonine, and tryptophan (LEAA+KTW), phenylalanine, histidine, and methionine (LEAA+FHM), or isoleucine, leucine, and valine

(LEAA+ILV), all with other AA equally adjusted to give 18%AA in total. Data (n=6 per group) are mean and SEM. Different than NAA: * P <0.05, **P<0.01, ***P<0.001. Different than LEAA: $^{\#}$P<0.05, $^{\#\#}$P<0.01, $^{\#\#\#}$P<0.001.

B: Energy expenditure of mice as in A.

C: Serum fibroblast growth factor 21 (FGF21) levels of mice as in A.

D: Insulin sensitivity index during fasting (ISI(f)) of mice as in A.

E: Feed efficiency of mice in response to a 3wk treatment with diets containing 18% from amino acids (AA; NAA), 4.5% essential AA (LEAA; as of diet E in Figure 2C), and diet singly with restricted amounts of lysine (LK), threonine (LT), and tryptophan (LW), all with other AA equally adjusted to give 18%AA in total. n=6 per group.

F: Energy expenditure of mice as in E.

G: Serum FGF21 levels of mice as in E.

H: ISI(f) of mice as in E.

I: Feed efficiency of mice in response to a 3wk treatment with diets containing 18% from amino acids (normal amino acid; NAA), 4.5% AA (LAA; as of diet B in Figure 2C), and LAA supplemented with threonine and tryptophan while keeping total AA at 4.5% (LAA(TW)). Date are mean and SEM (N=5 per group). Different than NAA: * P <0.05, **P<0.01, ***P<0.001. Different than LAA: $^{\#}$P<0.05, $^{\#\#}$P<0.01, $^{\#\#\#}$P<0.001.

J: Energy expenditure of mice as in E.

K: Serum FGF21 levels of mice as in E.

L: ISI(f) of mice as in E.

Supplementary Figure 3. Certain essential amino acids including Threonine and Tryptophan are sufficient and necessary for the systemic metabolic effects of dietary protein dilution. Related to Figure 3.

A: The change (Δ) in body mass of mice in response to a 3wk treatment with diets containing 18% from amino acids (normal amino acid; NAA), 4.5% essential AA (LEAA; as of diet E in Figure 2C), and LEAA supplemented with either lysine, threonine, and tryptophan (LEAA+KTW), phenylalanine, histidine, and methionine (LEAA+FHM), or isoleucine, leucine, and valine (LEAA+ILV), all with other AA equally adjusted to give 18%AA in total. Date are mean and SEM (n=6 per group). Different than diet NAA: * P <0.05, **P<0.01, ***P<0.001. Different than diet LEAA: $^{\#}$P<0.05, $^{\#\#}$P<0.01, $^{\#\#\#}$P<0.001.

B: The rate of food energy (E) intake during the metabolic cage housing of mice as in A.

C: The rate of O_2 consumption (VO_2) of mice as in A.

D: Fasting blood glucose of mice as in A.

E: Fasting serum insulin of mice as in A.

F: Blood glucose during fasting of mice in response to a 3wk treatment with diets containing 18% from amino acids (normal amino acid; NAA), 4.5% essential AA (LEAA; as of diet E in Figure 2C), and LEAA supplemented with either lysine (LEAA+K), threonine (LEAA+T), and tryptophan (LEAA+W), all with other AA equally adjusted to give 18%AA in total. n=6 per group.

G: Insulin sensitivity index during fasting (ISI(f)) of mice as in F.

H: Fasting blood glucose of mice as in F.

I: Fasting serum insulin of mice as in F.

J: The change (Δ) in body mass of mice in response to a 3wk treatment with diets containing 18% from amino acids (AA; NAA), 4.5% essential AA (LEAA; as of diet E in Figure 2C), and diet singly with restricted amounts of lysine (LK), threonine (LT), and tryptophan (LW), all with other AA equally adjusted to give 18%AA in total. Data are mean and SEM (n=6 per group). Different than NAA: * P <0.05, **P<0.01, ***P<0.001. Different than LEAA: $^{\#}$P<0.05, $^{\#\#}$P<0.01, $^{\#\#\#}$P<0.001.

K: The rate of food energy (E) intake during the metabolic cage housing of mice as in J.

L: The rate of O_2 consumption (VO_2) of mice as in J.

M: Fasting blood glucose of mice as in J.

N: Fasting serum insulin of mice as in J.

O: Feed efficiency of mice in response to a 6wk treatment with diets containing normal amount of methionine, threonine and tryptophan (100% MTW) or specifically reduced levels of these amino acids (20% MTW). n=11-12 per group. Data are mean and SEM. Different than 100% MTW: * P <0.05, **P<0.01, ***P<0.001.

P: The change (Δ) in body mass of mice as in P.

Q: Food energy (E) intake of mice as in P.

R: Serum FGF21 of mice as in P.

S: The change of body weight of mice in response to a 3wk treatment with diets containing 18% from amino acids (normal amino acid; NAA), 4.5% AA (LAA; as of diet B in Figure 2C), and LAA supplemented with threonine and tryptophan while keeping total AA at 4.5% (LAA(TW)). Data are mean and SEM (n=5 per group). Different than NAA: * P <0.05, **P<0.01, ***P<0.001. Different than LAA: $^{\#}$P<0.05, $^{\#\#}$P<0.01, $^{\#\#\#}$P<0.001.

T: The rate of food energy (E) intake during the metabolic cage housing of mice as in S.

U: The rate of O_2 consumption (VO_2) of mice as in S.

V: Fasting blood glucose of mice as in S.

W: Fasting serum insulin of mice as in S.

Figure 4. The systemic metabolic response to dietary AA restriction is conserved in mature male and female mice.

A: The change in body, fat, and lean mass of 6mo old male (shown left) mice in response to an 8wk treatment with diets containing 18% from amino acids (normal amino acid; NAA), 4.5% AA (LAA; as of diet B in Figure 2C), 4.5% essential AA (LEAA; as of diet E in Figure 2C), and a diet low in Threonine but with matching total AA to NAA (LT). Data are mean and SEM (n=5 per group). Different than NAA: ^{a}P <0.05, ^{aa}P<0.01, ^{aaa}P<0.001. Different than LAA: ^{b}P<0.05, ^{bb}P<0.01, ^{bbb}P<0.001. Different than LEAA: ^{c}P<0.05, ^{cc}P<0.01, ^{ccc}P<0.001.

B: The change in body, fat, and lean mass of 6mo old female (shown left) mice treated as in A.

C: Tissue weights of mice at the end of the treatment as in A.

D: Tissue weights of mice at the end of the treatment as in B.

E: Feed efficiency during the 8wk treatment of mice as in A.

F: Feed efficiency during the 8wk treatment of mice as in B.

G: Energy expenditure of mice as in A.

H: Energy expenditure of mice as in B.

I: Serum fibroblast growth factor 21 (FGF21) levels of mice as in A.

J: Serum FGF21 of mice as in B.

K: Insulin sensitivity index during fasting (ISI(f)) of mice as in A.

L: ISI(f) of mice as in B.

Supplementary Figure 4. The systemic metabolic response to dietary AA restriction is conserved in mature male and female mice. Related to Figure 4.

A: Body mass of 6mo old male (shown left) mice in response to an 8wk treatment with diets containing 18% from amino acids (normal amino acid; NAA), 4.5% AA (LAA; as of diet B in Figure 2C), 4.5% essential AA (LEAA; as of diet E in Figure 2C), and a diet low in Threonine but with matching total AA to NAA (LT). Data are mean and SEM (n=5 per group). Different than NAA: ^{a}P <0.05, ^{aa}P<0.01, ^{aaa}P<0.001. Different than LAA: ^{b}P<0.05, ^{bb}P<0.01, ^{bbb}P<0.001. Different than LEAA: ^{c}P<0.05, ^{cc}P<0.01, ^{ccc}P<0.001.

B: Body mass of 6mo old female (shown left) mice treated as in A.

C: The rate of food energy (E) intake of mice as in A.

D: The rate of food energy (E) intake of mice as in B.

E: Fasting blood glucose of mice as in A.

F: Fasting blood glucose of mice as in B.

G: Fasting plasma insulin levels of mice as in A.

H: Fasting plasma insulin levels of mice as in B.

I: Serum triglyceride levels of mice as in A.

J: Serum triglyceride levels of mice as in B.

K: Serum insulin-like growth factor 1 (IGF1) levels of mice as in A.

L: Serum IGF1 levels of mice as in B.

Figure 5. Threonine restriction is a common feature of other models of systemic AA restriction and retards obesity-induced metabolic dysfunction in mice.

A: Plasma threonine (THR) levels from young men on their prior normal diet (ND) and after 7d adaptation to a protein-restricted diet (PR) during an acute meal-tolerance test reflecting these diets. N=5/group. Data are mean and SEM. Main effect of diet: * P <0.05.

B: A scatter plot of the amino acid supply in the protein restricted diet (from A) versus the % amino acids found in the human exome. The line reflects the lowest slope of any EAA and intersects the AA threonine.

C: Hepatic portal vein serum amino acid (AA) concentrations in Slc6a19 knockout (-/-) or wildtype (+/+) littermate mice in the refed state on a standard control diet. N=5/group. Data are mean and SEM. Different than +/+: * P <0.05.

D: Plasma FGF21 levels from Slc6a19 knockout (-/-) or wildtype (+/+) littermate mice in the refed state following intraperitoneal administration of the amino acids threonine and tryptophan (TW), phenylalanine and histidine (FH), or vehicle (VEH: saline solution) on a standard control diet. N=5/group. Data are mean and SEM. Different than +/+: * P <0.05, **P<0.01, ***P<0.001. Different than VEH: $^{\#}$P<0.05, $^{\#\#}$P<0.01, $^{\#\#\#}$P<0.001.

E: Blood glucose levels during a 4 wk treatment of New Zealand Obese mice fed diets containing 18% from amino acids (normal amino acid; NAA) or a diet low in Threonine but with matching total AA to NAA (LT). Data are mean and SEM (N=8 per group). Different than NAA: * P <0.05, **P<0.01, ***P<0.001.

F: Serum triglyceride (TG) levels at the end of mice at the end of treatment as in E.

G: Serum fibroblast growth factor 21 (FGF21) levels of mice at the end of treatment as in E.

Supplementary Figure 5. Threonine restriction is a common feature of other models of systemic AA restriction and retards obesity-induced metabolic dysfunction in mice. Related to Figure 5.

A: Body mass during a 4 wk treatment of New Zealand Obese mice fed diets containing 18% from amino acids (normal amino acid; NAA) or a diet low in Threonine but with matching total AA to NAA (LT). Data are mean and SEM (N=8 per group). Different than NAA: * P <0.05, **P<0.01, ***P<0.001.

B: Tissue mass' of mice at the end of treatment as in A.

Figure 6. Liver-derived fibroblast growth factor 21 is necessary for the systemic metabolic remodelling with dietary threonine restriction.

A: Serum fibroblast growth factor 21 (FGF21) levels of Fgf21fl/fl mice at the end of an 8wk treatment with diets containing 18% from amino acids (AA; NAA) or low threonine with other AA equally adjusted to give 18%AA in total (LT); with pre-treatment with adeno-associated viruses to express Cre-recombinase (AAV-CRE) or green fluorescent protein (AAV-GFP) in an hepatocyte-selective manner. Data are mean and SEM (n=6-8 per group). Different than NAA: * P <0.05, **P<0.01, ***P<0.001. Different than AAV-GFP: $^{\#}$P<0.05, $^{\#\#}$P<0.01, $^{\#\#\#}$P<0.001.

B: Feed efficiency during the 8wk treatment of mice as in A.

C: Energy expenditure of mice as in A.

D: Insulin sensitivity index during fasting (ISI(f)) of mice as in A.

Supplementary Figure 6. Liver-derived fibroblast growth factor 21 is necessary for the systemic metabolic remodelling with dietary threonine restriction. Related to Figure 6.

A: Body mass of Fgf21fl/fl mice during an 8wk treatment with diets containing 18% from amino acids (AA; NAA) or low threonine with other AA equally adjusted to give 18%AA in total (LT); with pre-treatment with adeno-associated viruses to express Cre-recombinase (AAV-CRE) or green fluorescent protein (AAV-GFP) in an hepatocyte-selective manner. Data are mean and SEM (n=6-8 per group). Different than NAA: * P <0.05, **P<0.01, ***P<0.001. Different than AAV-GFP: $^{\#}$P<0.05, $^{\#\#}$P<0.01, $^{\#\#\#}$P<0.001.

B: The change of body mass of mice over the 8wk treatment period of mice as in A.

C: Tissue mass' of mice at the end of treatment as in A.

D: The rate of O_2 consumption (VO_2) of mice as in A.

E: The rate of food energy (E) intake of mice as in A.

F: Fasting blood glucose of mice as in A.

G: Fasting plasma insulin levels of mice as in A.

H: Serum triglyceride levels of mice as in A.

Figure 7. Enforced hepatic threonine biosynthetic capacity reverses the systemic metabolic effects to dietary threonine restriction.

A: Feed efficiency of mice in response to a 3wk treatment with diets containing 18% from amino acids (normal amino acid; NAA; yellow bars) and a diet with restricted amounts of threonine (LT; green bars), following prior treatments with adeno-associated viruses to transduce the liver to express yeast threonine biosynthetic enzymes (AAV-yTHR1+THR4) or a negative control (AAV-GFP). Data are mean and SEM (N= 6 per group). Different than diet NAA: * P <0.05, **P<0.01, ***P<0.001. Different than AAV-GFP: $^{\#}$P<0.05, $^{\#\#}$P<0.01, $^{\#\#\#}$P<0.001.

B: Energy expenditure of mice as in A.

C: Serum fibroblast growth factor 21 (FGF21) levels of mice as in A.

D: Insulin sensitivity index during fasting (ISI(f)) of mice as in A.

Supplementary Figure 7. Enforced hepatic threonine biosynthetic capacity reverses the systemic metabolic effects to dietary threonine restriction. Related to Figure 7.

A: The liver expression of yTHR1 and yTHR4 as revealed by proteomics analyses of mice in response to a 3wk treatment with diets containing 18% from amino acids (normal amino acid; NAA; yellow bars) and a diet with restricted amounts of threonine (LT; green bars), following prior treatments with adeno-associated viruses to transduce the liver to express yeast threonine biosynthetic enzymes (AAV-yTHR1+THR4) or a negative control (AAV-GFP). Data are mean and SEM (N= 6 per group). Different than diet NAA: * P <0.05, **P<0.01, ***P<0.001. Different than AAV-GFP: $^{\#}$P<0.05, $^{\#\#}$P<0.01, $^{\#\#\#}$P<0.001.

B: The liver threonine concentration as revealed by quantitative metabolomics of mice as in A.

C: The rate of food energy (E) intake during the metabolic cage housing of mice as in A.

D: The change (Δ) in body mass of as in A.

E: The rate of O_2 consumption (VO_2) of mice as in A.

F: Fasting blood glucose of mice as in A.

G: Fasting serum insulin of mice as in A.

Figure 1

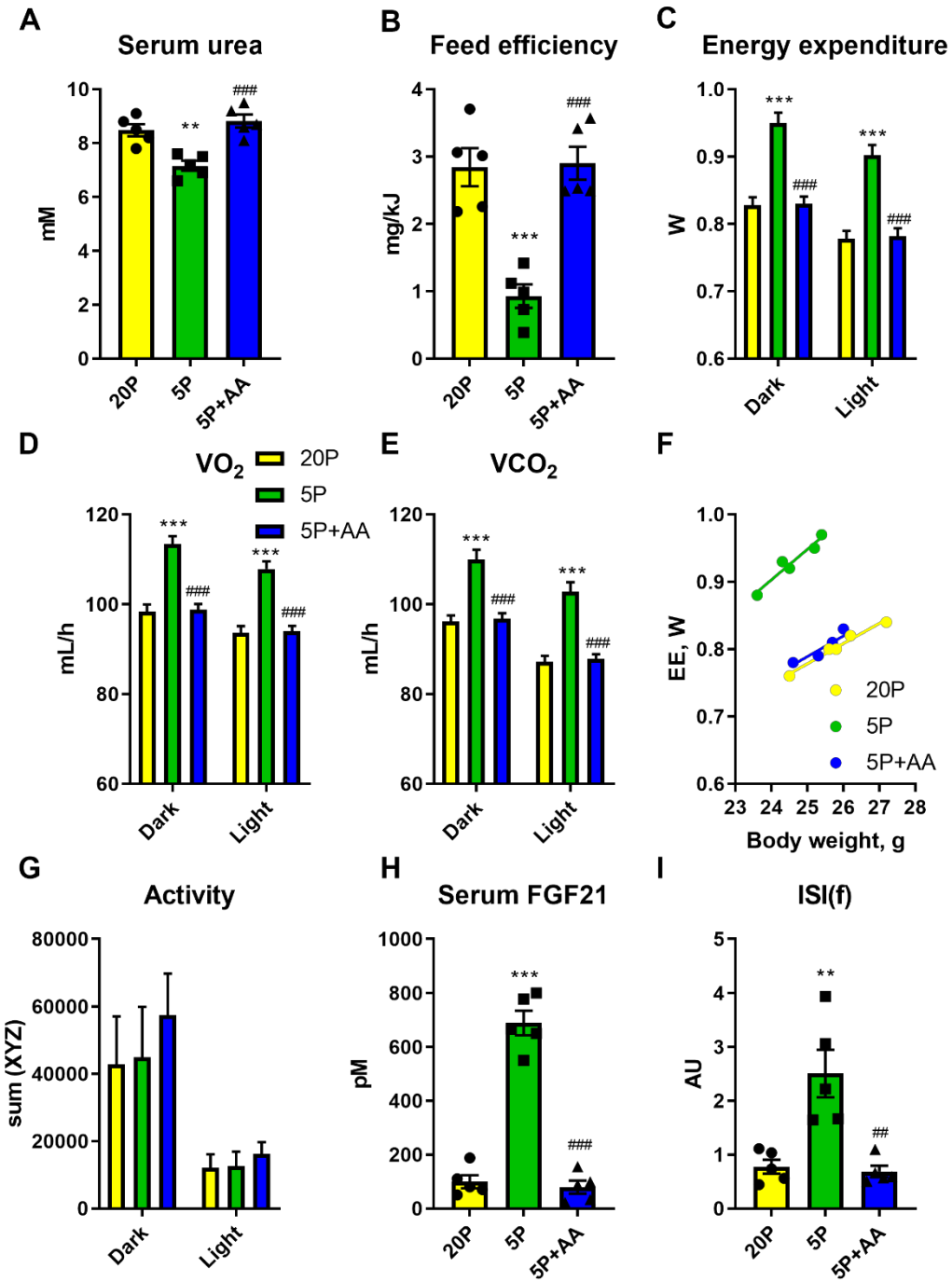
A
Serum urea
mM
B
Feed efficiency
mg/kJ
C
Energy expenditure
W
Dark
Light
20P
5P
5P+AA
D
VO2
mL/h
E
VCO2
mL/h
F
EE, W
Body weight, g
G
Activity
sum (XYZ)
H
Serum FGF21
pM
I
ISI(f)
AU

Figure S1

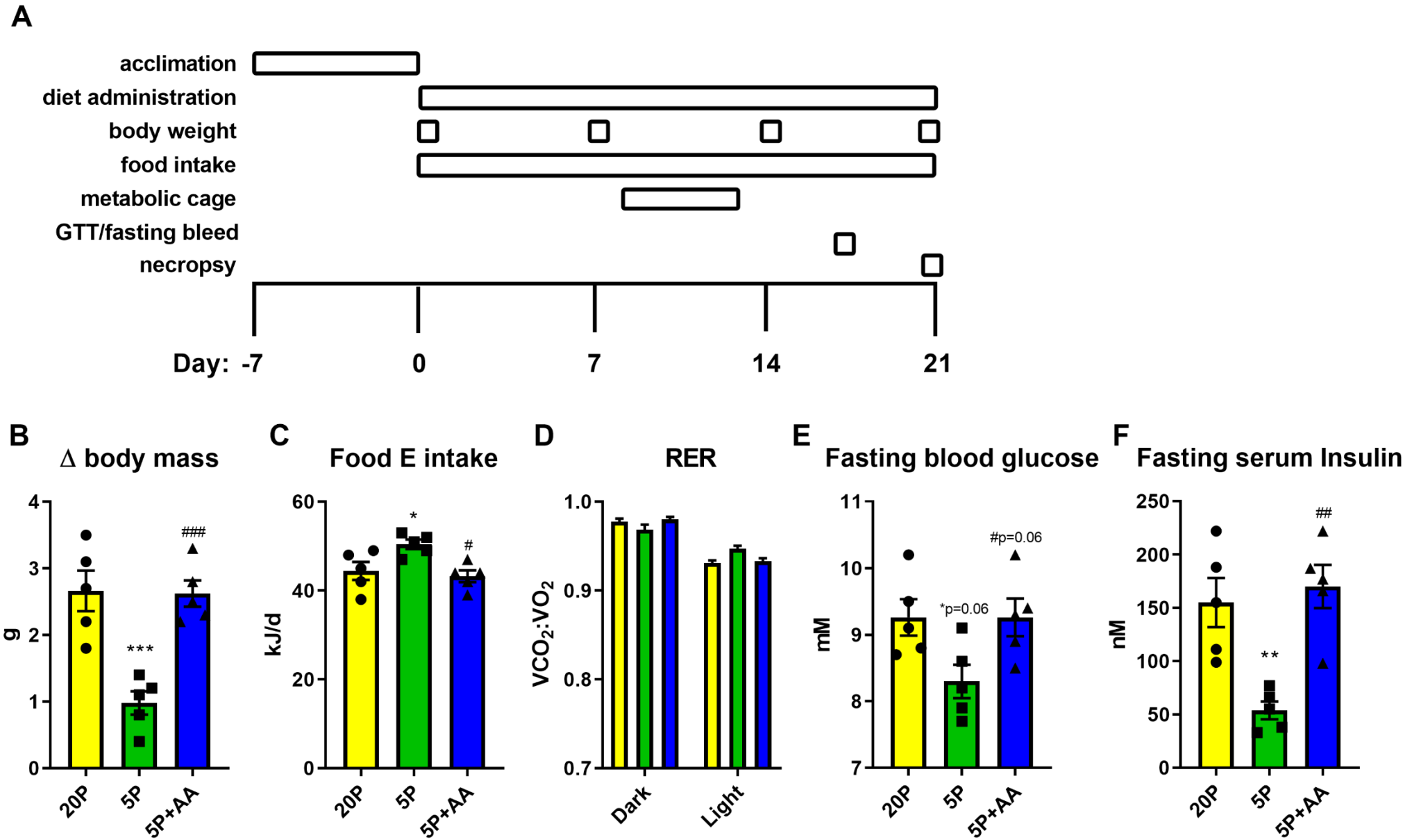
A
acclimation
diet administration
body weight
food intake
metabolic cage
GTT/fasting bleed
necropsy
Day: -7
0
7
14
21
B
Δ body mass
g
***
###
20P
5P
5P+AA
C
Food E intake
kJ/d
*
#
D
RER
VCO2:VO2
Dark
Light
E
Fasting blood glucose
mM
*p=0.06
#p=0.06
F
Fasting serum Insulin
nM
**
##

Figure 2

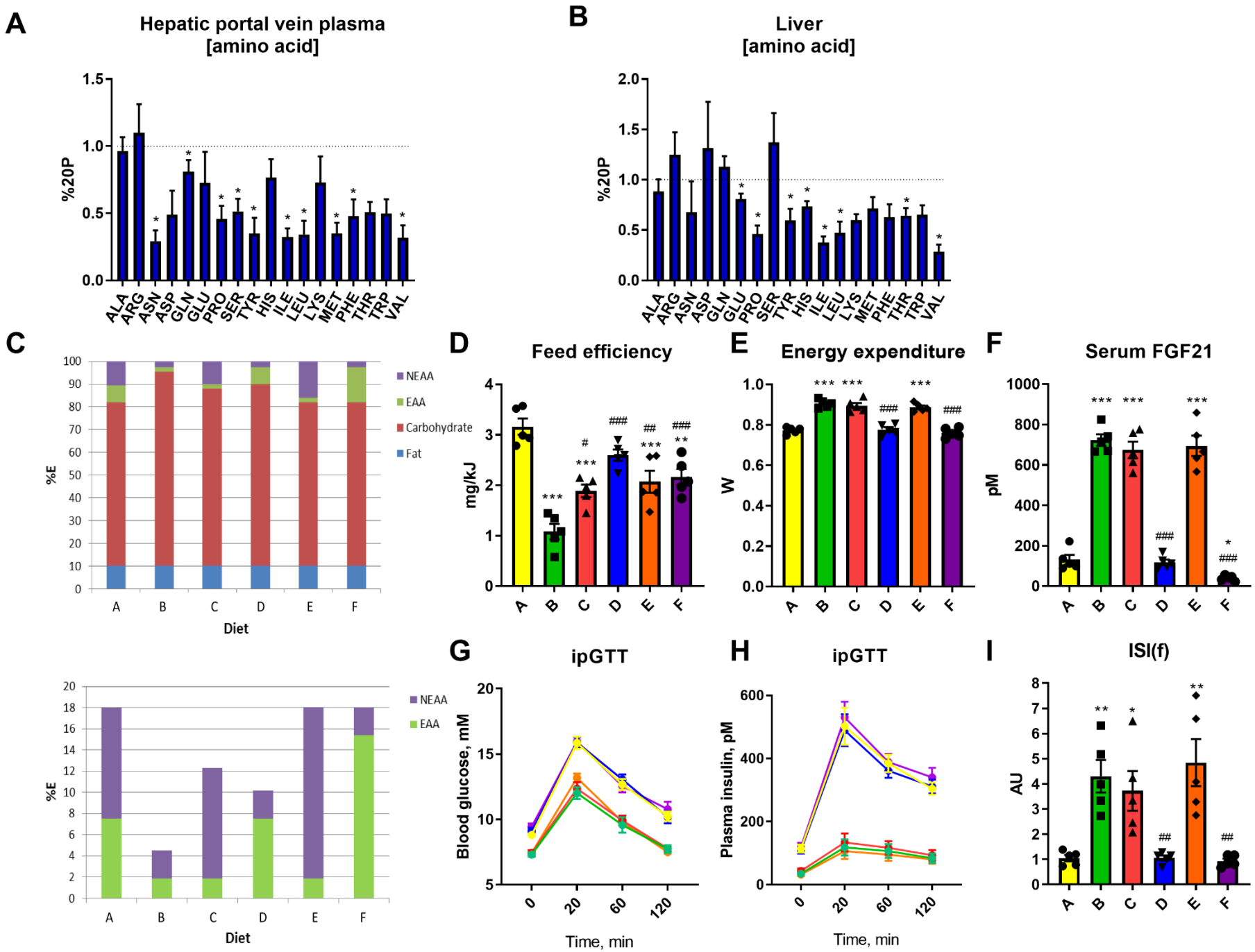
A
Hepatic portal vein plasma
[amino acid]
%20P
ALA ARG ASN ASP GLN GLU PRO SER TYR HIS ILE LEU LYS MET PHE THR TRP VAL
B
Liver
[amino acid]
%20P
ALA ARG ASN ASP GLN GLU PRO SER TYR HIS ILE LEU LYS MET PHE THR TRP VAL
C
%E
NEAA
EAA
Carbohydrate
Fat
A B C D E F
Diet
%E
NEAA
EAA
A B C D E F
Diet
D
Feed efficiency
mg/kJ
A B C D E F
E
Energy expenditure
W
A B C D E F
F
Serum FGF21
pM
A B C D E F
G
ipGTT
Blood glucose, mM
0 20 60 120
Time, min
H
ipGTT
Plasma insulin, pM
0 20 60 120
Time, min
I
ISI(f)
AU
A B C D E F

Figure S2

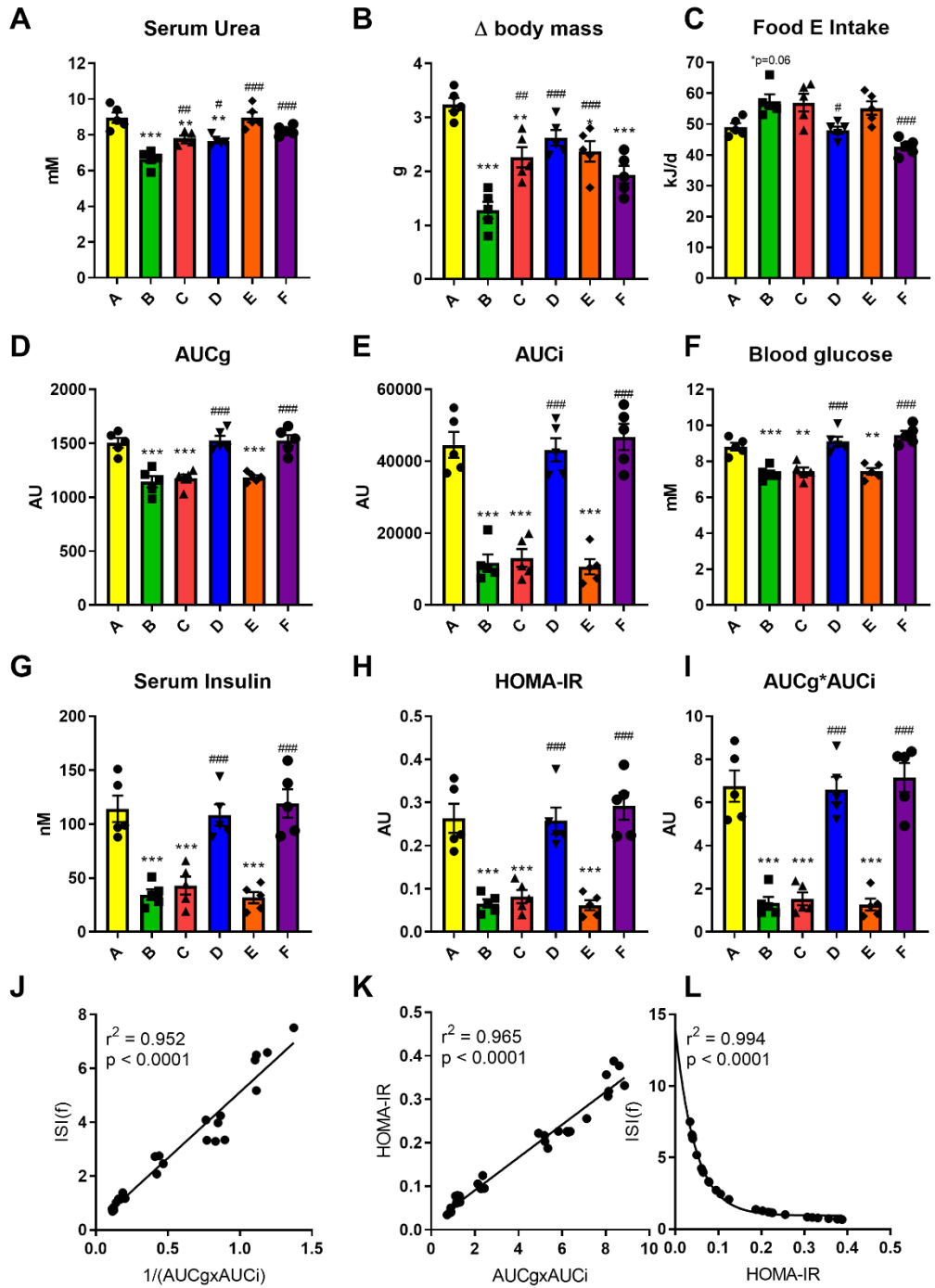
A
Serum Urea
mM
B
Δ body mass
g
C
Food E Intake
*p=0.06
kJ/d
D
AUCg
AU
E
AUCi
AU
F
Blood glucose
mM
G
Serum Insulin
nM
H
HOMA-IR
AU
I
AUCg*AUCi
AU
J
r2 = 0.952
p < 0.0001
ISI(f)
1/(AUCgxAUCi)
K
r2 = 0.965
p < 0.0001
HOMA-IR
AUCgxAUCi
L
r2 = 0.994
p < 0.0001
ISI(f)
HOMA-IR

Figure 3

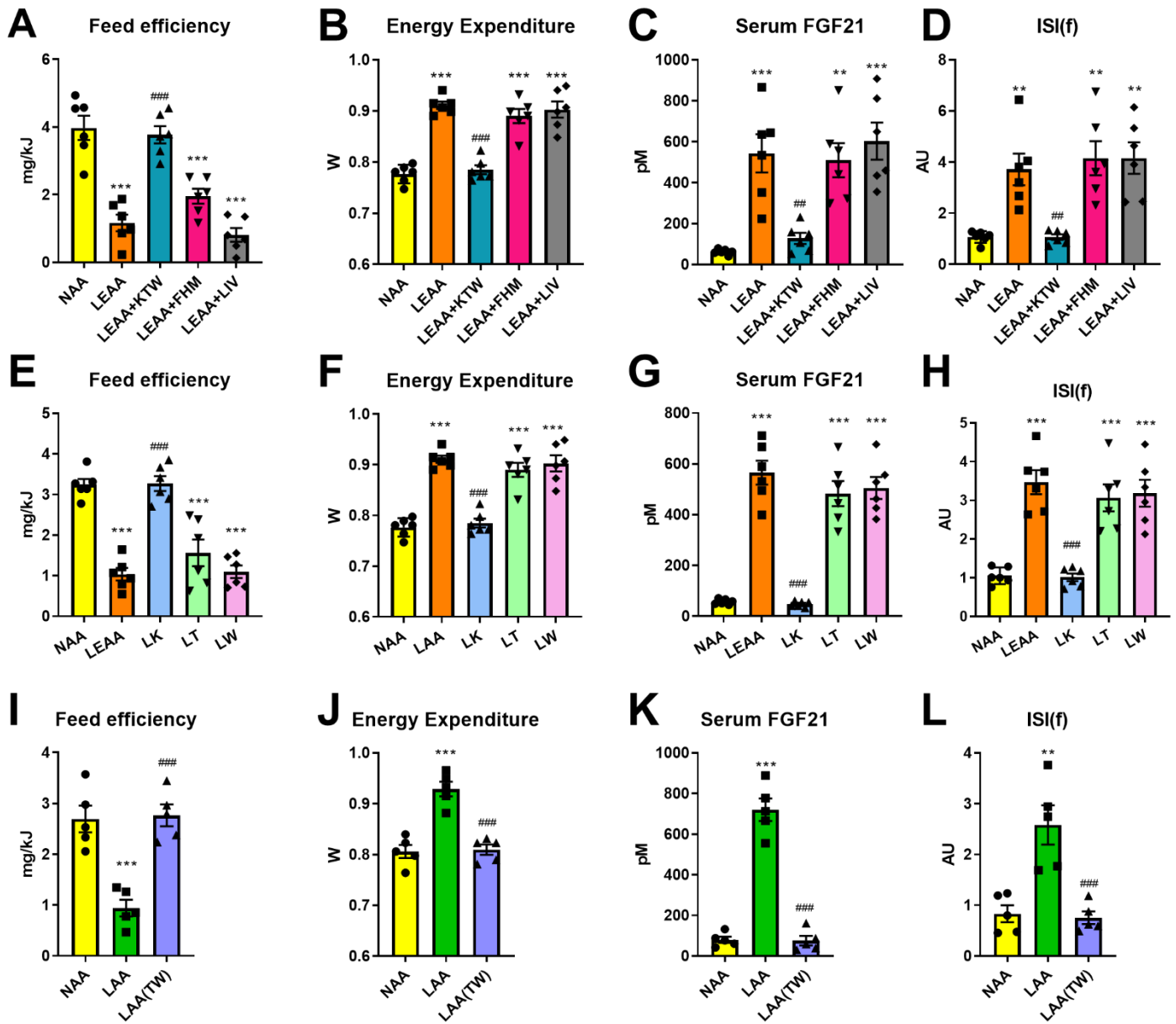
A
Feed efficiency
mg/kJ
NAA
LEAA
LEAA+KTW
LEAA+FHM
LEAA+LIV
B
Energy Expenditure
W
C
Serum FGF21
pM
D
ISI(f)
AU
E
Feed efficiency
mg/kJ
NAA
LEAA
LK
LT
LW
F
Energy Expenditure
W
NAA
LAA
LK
LT
LW
G
Serum FGF21
pM
H
ISI(f)
AU
I
Feed efficiency
mg/kJ
NAA
LAA
LAA(TW)
J
Energy Expenditure
W
K
Serum FGF21
pM
L
ISI(f)
AU

Figure S3

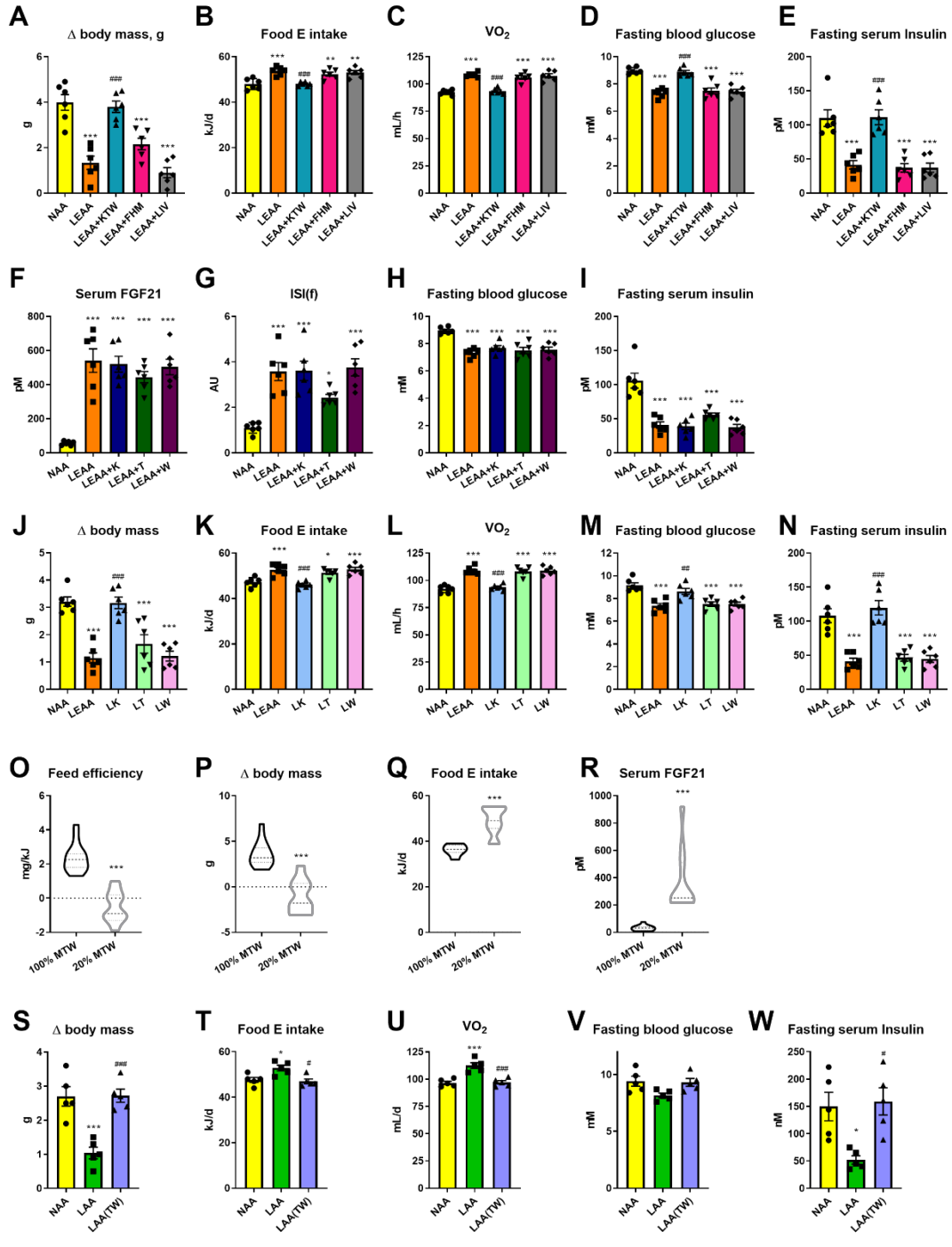
A
Δ body mass, g
g
NAA
LEAA
LEAA+KTW
LEAA+FHM
LEAA+LIV
B
Food E intake
kJ/d
C
VO2
mL/h
D
Fasting blood glucose
mM
E
Fasting serum Insulin
pM
F
Serum FGF21
pM
NAA
LEAA
LEAA+K
LEAA+T
LEAA+W
G
ISI(f)
AU
H
Fasting blood glucose
mM
I
Fasting serum insulin
pM
J
Δ body mass
g
NAA
LEAA
LK
LT
LW
K
Food E intake
kJ/d
L
VO2
mL/h
M
Fasting blood glucose
mM
N
Fasting serum insulin
pM
O
Feed efficiency
mg/kJ
100% MTW
20% MTW
P
Δ body mass
g
Q
Food E intake
kJ/d
R
Serum FGF21
pM
S
Δ body mass
g
NAA
LAA
LAA(TW)
T
Food E intake
kJ/d
U
VO2
mL/d
V
Fasting blood glucose
mM
W
Fasting serum Insulin
nM

Figure 4

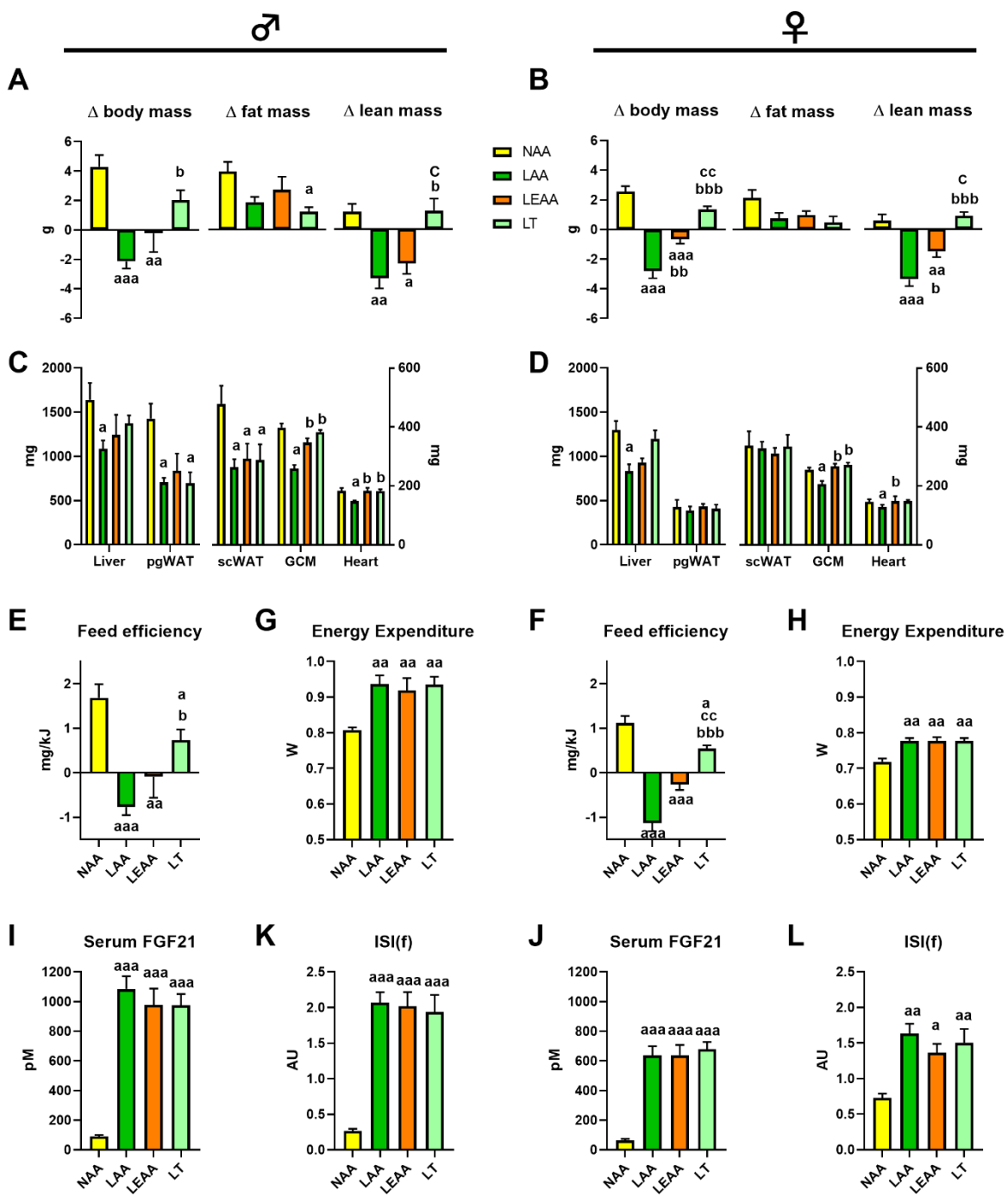
♂
♀
A
B
Δ body mass
Δ fat mass
Δ lean mass
NAA
LAA
LEAA
LT
g
C
D
mg
mg
Liver
pgWAT
scWAT
GCM
Heart
E
F
Feed efficiency
mg/kJ
G
H
Energy Expenditure
W
I
J
Serum FGF21
pM
K
L
ISI(f)
AU

Figure S4

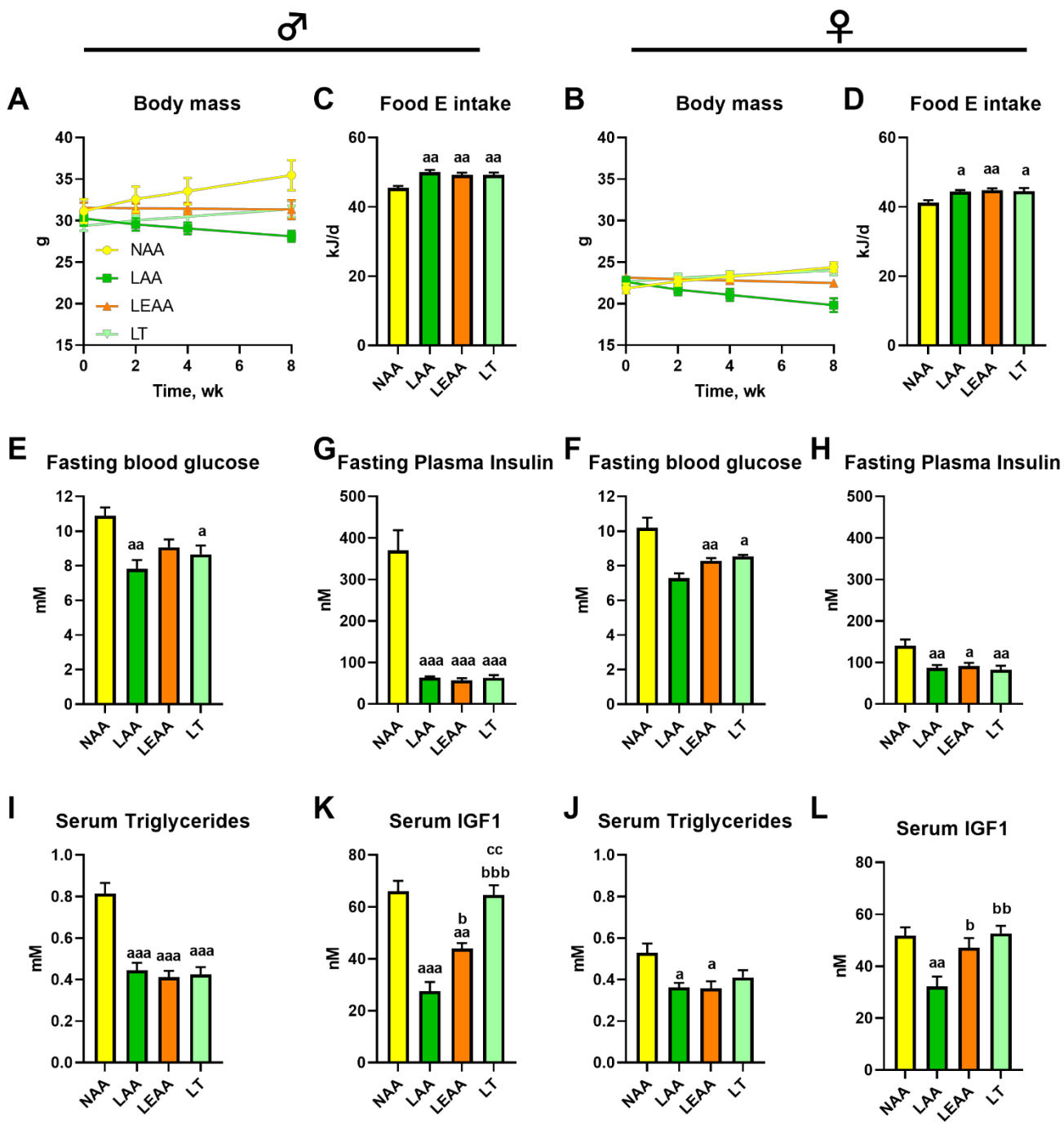
♂
♀
A
Body mass
g
Time, wk
NAA
LAA
LEAA
LT
C
Food E intake
kJ/d
aa aa aa
B
Body mass
g
Time, wk
D
Food E intake
kJ/d
a aa a
E
Fasting blood glucose
mM
aa a
G
Fasting Plasma Insulin
nM
aaa aaa aaa
F
Fasting blood glucose
mM
aa a
H
Fasting Plasma Insulin
nM
aa a aa
I
Serum Triglycerides
mM
aaa aaa aaa
K
Serum IGF1
nM
aaa b aa cc bbb
J
Serum Triglycerides
mM
a a
L
Serum IGF1
nM
aa b bb

Figure 5

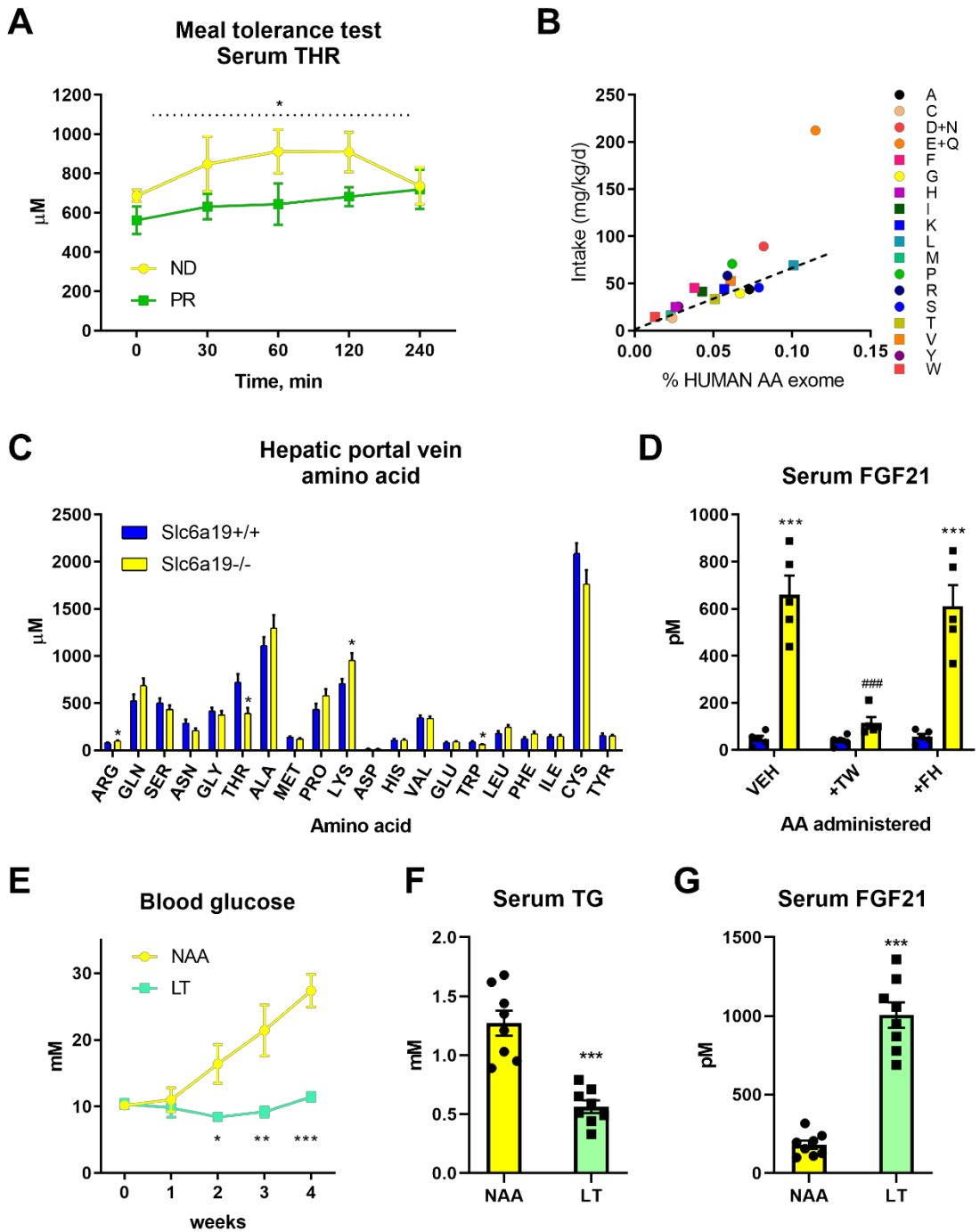
A
Meal tolerance test
Serum THR
µM
ND
PR
Time, min
B
Intake (mg/kg/d)
% HUMAN AA exome
A
C
D+N
E+Q
F
G
H
I
K
L
M
P
R
S
T
V
Y
W
C
Hepatic portal vein
amino acid
Slc6a19+/+
Slc6a19-/-
µM
ARG GLN SER ASN GLY THR ALA MET PRO LYS ASP HIS VAL GLU TRP LEU PHE ILE CYS TYR
Amino acid
D
Serum FGF21
pM
VEH
+TW
+FH
AA administered
E
Blood glucose
NAA
LT
mM
weeks
F
Serum TG
mM
NAA
LT
G
Serum FGF21
pM
NAA
LT

SF5

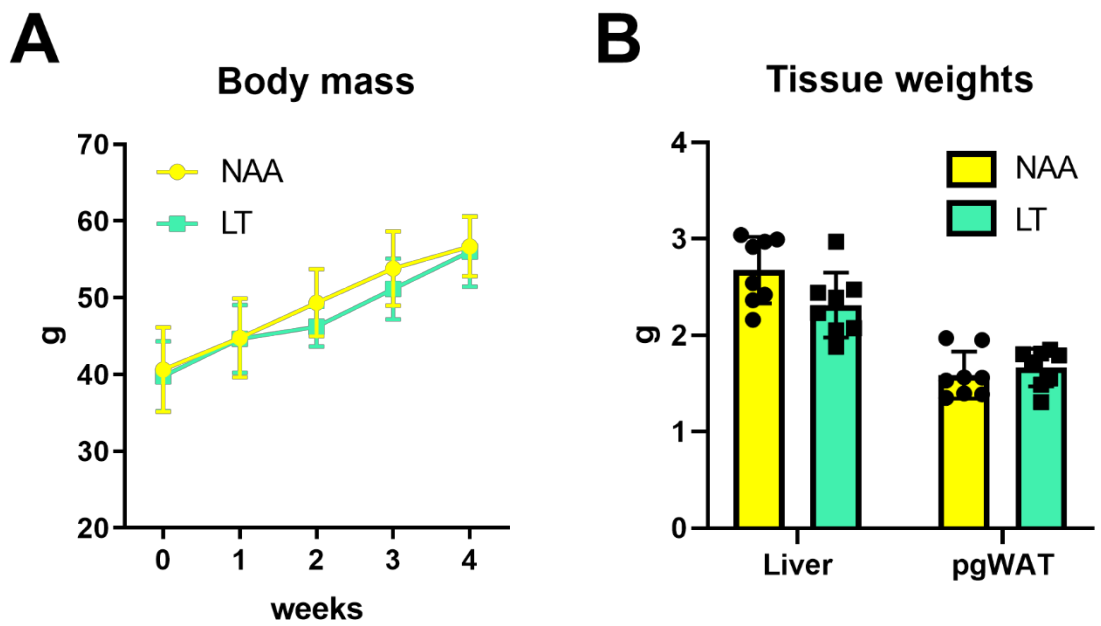
A
Body mass
70
60
50
40
30
20
g
NAA
LT
0
1
2
3
4
weeks
B
Tissue weights
4
3
2
1
0
g
NAA
LT
Liver
pgWAT

Figure 6

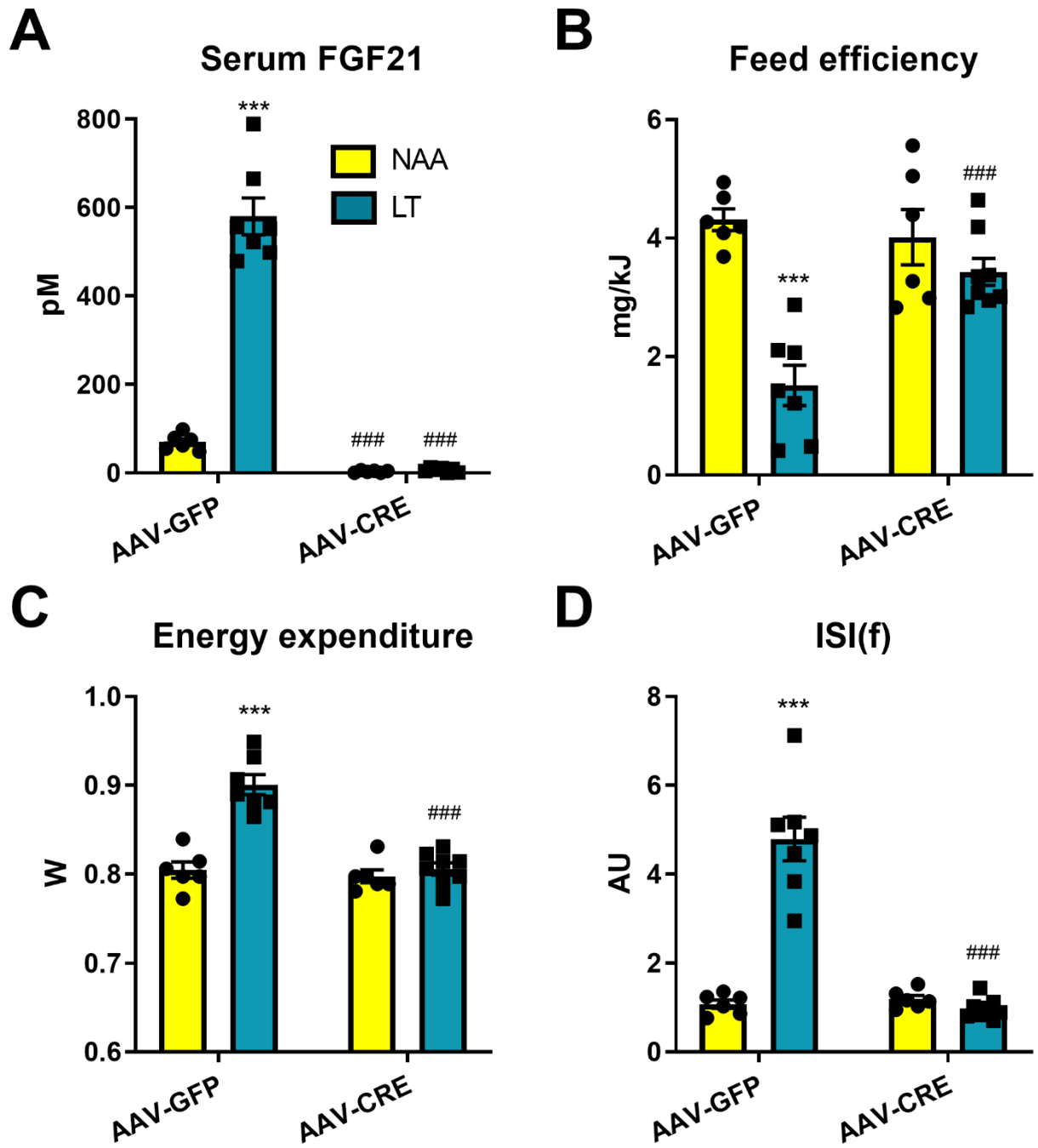
A
Serum FGF21
pM
800
600
400
200
0
NAA
LT
***
###
###
AAV-GFP
AAV-CRE
B
Feed efficiency
mg/kJ
6
4
2
0
***
###
AAV-GFP
AAV-CRE
C
Energy expenditure
W
1.0
0.9
0.8
0.7
0.6
***
###
AAV-GFP
AAV-CRE
D
ISI(f)
AU
8
6
4
2
0
***
###
AAV-GFP
AAV-CRE

Figure S6

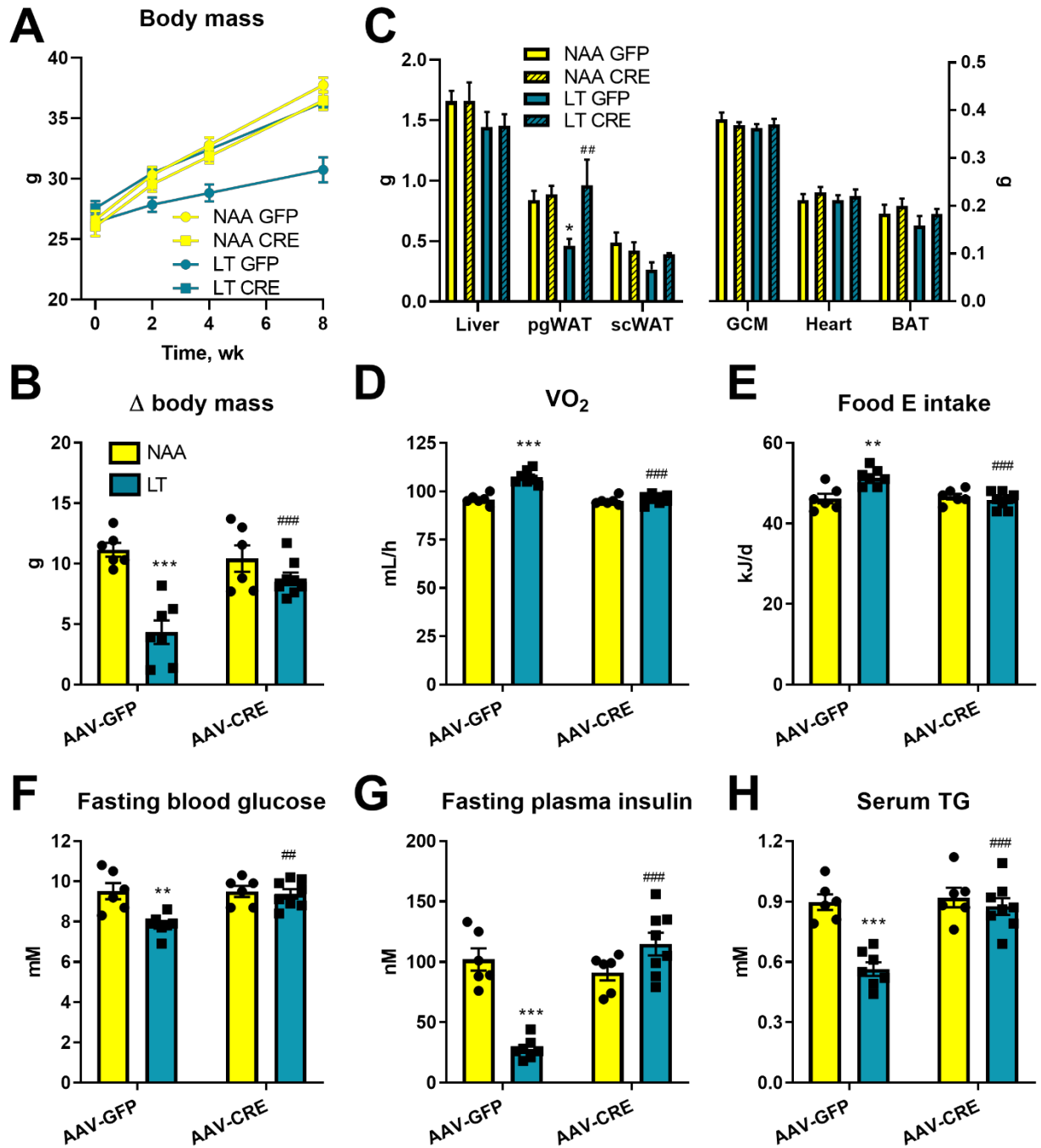
A
Body mass
g
Time, wk
NAA GFP
NAA CRE
LT GFP
LT CRE
C
NAA GFP
NAA CRE
LT GFP
LT CRE
Liver
pgWAT
scWAT
GCM
Heart
BAT
B
Δ body mass
NAA
LT
AAV-GFP
AAV-CRE
D
VO2
mL/h
E
Food E intake
kJ/d
F
Fasting blood glucose
mM
G
Fasting plasma insulin
nM
H
Serum TG
mM

Figure 7

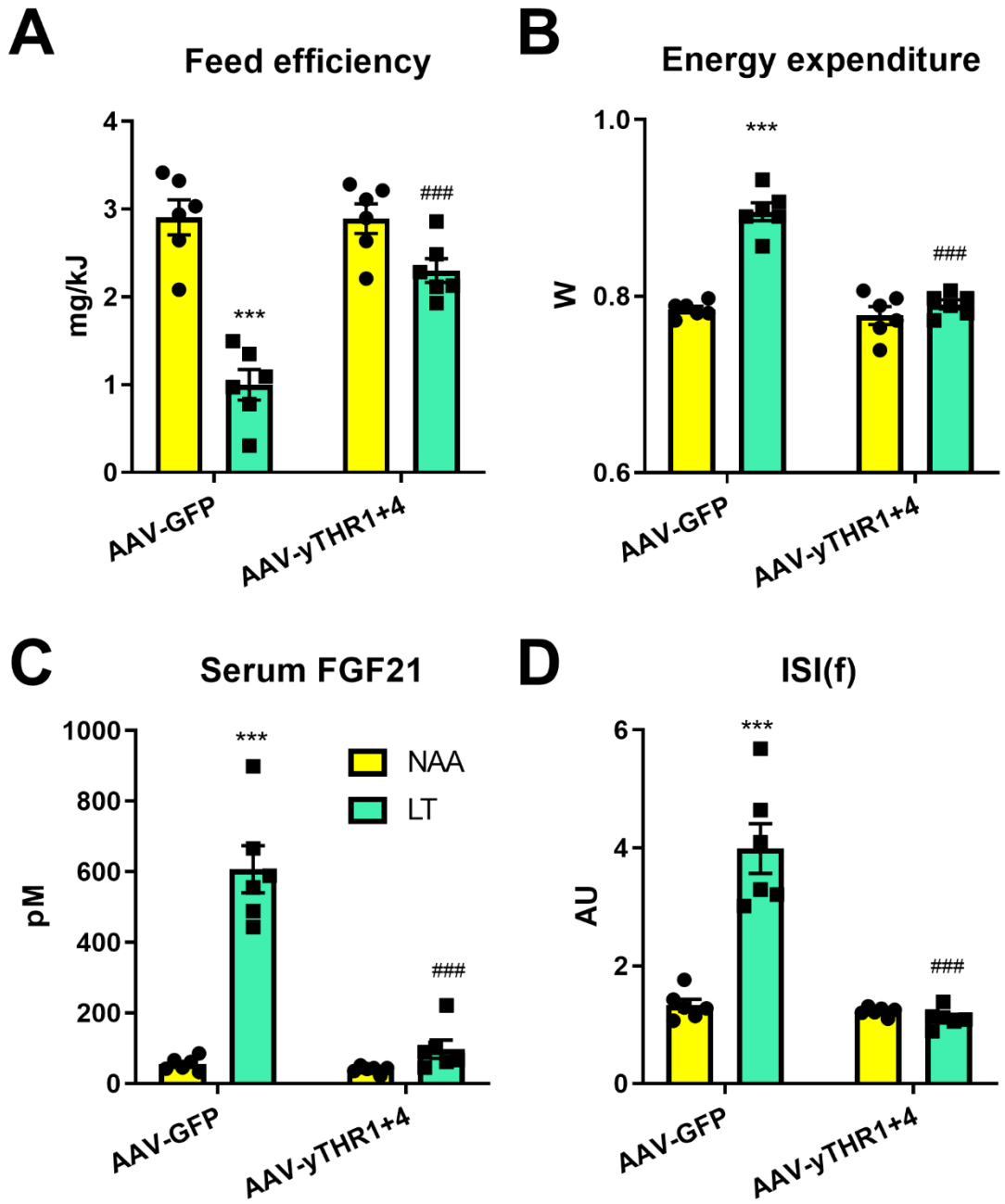
A
Feed efficiency
mg/kJ
4
3
2
1
0
***
###
AAV-GFP
AAV-yTHR1+4
B
Energy expenditure
W
1.0
0.8
0.6
***
###
AAV-GFP
AAV-yTHR1+4
C
Serum FGF21
pM
1000
800
600
400
200
0
***
###
NAA
LT
AAV-GFP
AAV-yTHR1+4
D
ISI(f)
AU
6
4
2
0
***
###
AAV-GFP
AAV-yTHR1+4

Figure S7

A

Protein	No. of identified unique peptides from sample	
	AAV-GFP	AAV-yTHR1+4
yTHR1	0	14
yTHR4	0	15